Master's thesis

NTNU
Norwegian University of Science and Technology
Faculty of Engineering
Department of Energy and Process Engineering

Rinaldi Anwar

Model for severe riser slugging in Phyton

Master's thesis in Natural Gas Technology
Supervisor: Ole Jørgen Nydal
June 2020

NTNU
Norwegian University of
Science and Technology

Rinaldi Anwar

Model for severe riser slugging in Phyton

Master's thesis in Natural Gas Technology
Supervisor: Ole Jørgen Nydal
June 2020

Norwegian University of Science and Technology
Faculty of Engineering
Department of Energy and Process Engineering

NTNU
Norwegian University of
Science and Technology

Summary

Severe slugging is the condition at which the liquid slugs are formed and violently blow out from the riser. It may lead to an unstable flow rate, causing the fluctuation of the gas production. Thus, it should be avoided to prevent operational problems in the field. One of the solutions is by using the multiphase dynamic flow simulators. This project aims to implement a Graphical User Interface (GUI) of a simplified severe slugging model. The work is based on a previous Matlab implemented in Python language and specialization project. To achieve the objectives, the project was structured into three parts. The project initiated with reviewing the previous severe slugging calculation, review well-known transition criteria. The second part of the project was implementing a GUI of the model by considering several main features such as plot results, export, flow regime transition map and severe slugging stability map. In the final step, a comparison between flow regime maps and severe slugging stability maps was conducted. The project showed the successful design and implementation of GUI that can simulate the flow regime map and severe slugging stability map.

Preface

This thesis has been conducted as the final part of master's degree program in Natural Gas Technology, Department of Energy and Process Engineering at Norwegian University of Science and Technology (NTNU) in Spring 2020. The topic of this thesis is about the Model of Severe Slugging in Python.

I received a lot of support and guidance through this thesis project as well as along my studies at Natural Gas Technology department and NTNU. Therefore, I would like to express my gratitude to my project supervisor, Professor Ole Jørgen Nydal, for all the knowledge, guidance and opportunities to learn the topic so that I am able to finish the project.

I would like to also thank Stack Overflow Community for allowing me to study Python and providing me the guidance and advice related to problems that I faced during the python programming for this project. At last, I could not successfully finish my master also without all individuals who in one way or another contributed to the completion of this thesis whom I would like to also thank and appreciate.

Trondheim, June 2020

Rinaldi Anwar

Table of Contents

List of Tables

List of Figures

Abbreviations

n	=	Number of step for numerical calculation
A	=	Area
dt	=	Time difference for numerical calculation
t_s	=	Residence time of a slug passing a cross-section of the pipe
t_b	=	Residence time of a bubble passing a cross-section of the pipe
ρ_L	=	Liquid density (isothermal)
μ_L	=	Liquid viscosity (isothermal)
C_0	=	Coefficient for bubble velocity
R	=	Gas constant
T	=	Temperature
MW	=	Molecular weight
D	=	Pipe diameter
D_h	=	Hydraulic diameter
D_g	=	Gas diameter in annular
F_B	=	Buoyancy force
F_T	=	Turbulent force
H	=	Liquid hold-up
h	=	Liquid height
L	=	Length
F_r	=	Froude number
L_L	=	Pipeline length
L_R	=	Riser length
θ	=	Pipeline inclination
σ_{gl}	=	Gas-liquid surface tension
P_{normal}	=	Pipeline inlet pressure
P_{out}	=	Riser outlet pressure
U_{sgin}	=	Gas phase inlet superficial velocity
U_{slin}	=	Liquid phase inlet superficial velocity
C_{valve}	=	Valve constant
ρ_{gR}	=	Gas density in the riser
ρ_m	=	mixed density in the riser
ρ_{gL}	=	Gas density in the pipeline
ρ_g	=	Gas density
ρ_l	=	Liquid density
α	=	Void fraction
α_s	=	Void fraction in the slug
α_b	=	Void fraction in the bubble
β	=	Wet perimeter half-angle
μ	=	Dynamic viscosity

z_L	=	Liquid level in the pipeline
z_R	=	Riser mixture level
g	=	Gravity
Re	=	Reynolds number
z_L	=	Mixture level in the pipeline
ψ	=	Additional friction
λ	=	Friction factor
δ	=	Dimensionless film thickness
K	=	Damping factor
τ_{gw}	=	Shear stress gas wall
τ_{lw}	=	Shear stress liquid wall
τ_i	=	Shear stress gas-liquid interface
S_{gw}	=	Gas wall perimeter
S_{lw}	=	Liquid wall perimeter
S_i	=	Gas liquid interfacial perimeter
SF	=	Slug fraction
S_D	=	Gas–liquid distribution slip in slug
U_{Level}	=	Liquid level velocity in the pipeline
U_g	=	Gas velocity
U_m	=	Mixture velocity
U_{sg}	=	Superficial gas velocity
U_{sl}	=	Superficial liquid velocity
U_{gs}	=	Gas velocity in the slug
U_{gb}	=	Gas velocity in the bubble
U_{ls}	=	Liquid velocity in the slug
U_{lb}	=	Liquid velocity in the bubble
U_b	=	Bubble front propagation velocity
U_f	=	Slug front velocity
U_{0s}	=	Vertical gas drift velocity in slug
U_0	=	Drift velocity of bubble in stagnant liquid

Chapter 1

Introduction

1.1 Background

Severe riser slugging also referred to as terrain slugging, is the phenomenon where large liquid slugs are formed in risers and violently blow out periodically. This phenomenon is highly undesirable due to high pressure and flow rate oscillation. The fluctuation of gas production may cause flaring and reduce the production capacity of the field [Jansen et al. (1996)]. Severe slugging is an operational problem that can be avoided. To prevent the occurrence of severe slugging, a hydrodynamic model of severe slugging can be used to design a new pipeline system or adjust the operation of an existing system. The development of flow simulators such as OLGA and LedaFlow are available for multiphase dynamic simulation. The simplified dynamic model can be constructed for the simple flowline-riser system. The model can be useful for sensitivity analysis of various parameters such as diameter, inclination, lengths, pressure, etc. The model was developed on basic physical principles and limited to how the slug generated at the base of the riser.

1.2 Objective

The objective of this project is to build a Graphical User Interface (GUI) of severe slugging stability map and severe slugging generating map. The work is a continuation of the specialization project. The project was divided into several tasks:

1. Review a previous Matlab implementation for flow regime map
2. Design the GUI for the flow regime map
3. Compare the result from generating map and severe slugging stability.

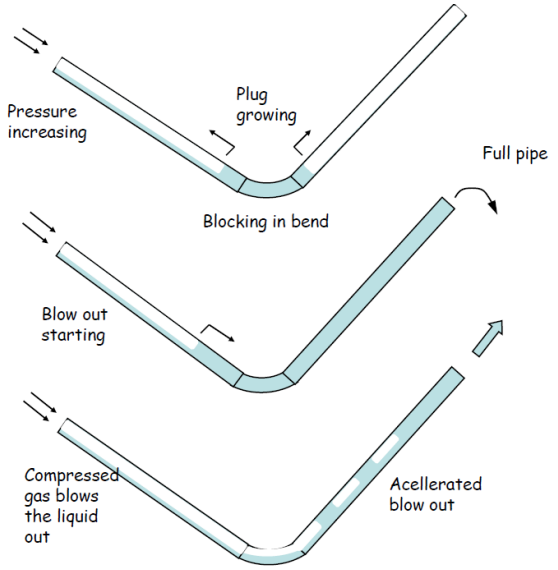

Figure 1.1: Severe slugging mechanism [Nydal (2019)].

1.3 Severe Slugging Mechanism

Severe slugging occurs when there is a low point (downward upstream and upward downstream) for liquid accumulation in the pipeline, upstream stratified flows, sufficient upstream gas compressibility, and suitable flow rates. The severe slugging phenomenon consists of a blowout, slug formation, gas compression, and slug production. The cycle of severe slugging starts at the gas production continues until the gas velocity insufficient to support liquid on the riser wall. The liquid begins to fall downward and accumulated until it blocked the entrance of the riser (slug generation). After the liquid level reaches the top of the riser, the pressure base of the riser still increases due to gas compressibility until maximum value (gas compression). The bubble region of the slug starts to penetrate until the bubble enters the separator. The liquid slug just exited the riser to the separator. The gas that blocked at the base of riser starts to expand rapidly carrying liquid droplet to the separator (blowout), and the cycle repeated. The mechanism is illustrated in **Fig. 1.1**. The severe slugging generating map can be achieved from the experiment illustrated in **Fig. 1.2**. The difference between severe slugging and the normal slug is characterized by the generation of liquid slugs at the base of the riser while normal slug is generated along the length of the pipeline [Schmidt et al. (1980)]. The generating map has a similar purpose as a flow regime map which able to predict the flow regime scenario at certain velocities.

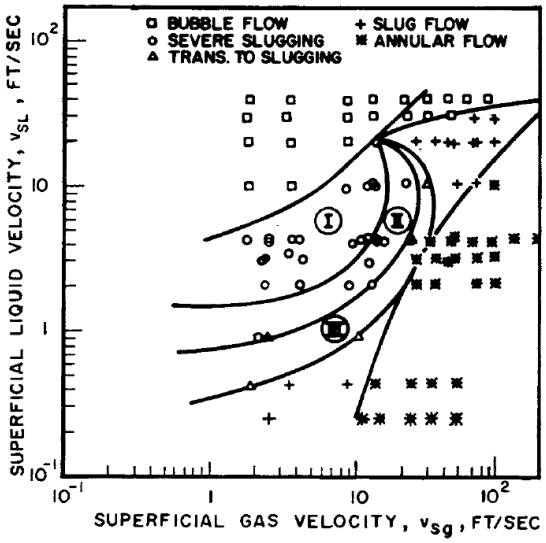

Figure 1.2: Severe slugging generating map at -5 pipeline inclination [Schmidt et al. (1980)].

1.4 Severe Slugging Prevention

Based on field measurements from the Gulf of Mexico, a decline in flow rate between the subsea tree and the riser causes the slugging [Kashou (1996)]. Severe slugging can generate slug length one or more of the riser length [Schmidt et al. (1985)]. A slug catcher is used to process severe slugging or slugs. The process can be challenging to implement when the size of the slugs is above the separator capacity which leads to liquid carry-over. There are several attempts to control and eliminate severe slugging phenomenon. Some of severe slugging elimination techniques are shown on **Table. 1.1** [Yocum et al. (1973); Tengesdal et al. (2003); De Salis et al. (1996)].

1.5 Software

In this section, the software that is used for this project is described. The main purpose of the software is to create added features for the GUI of the severe slugging model.

1.5.1 Python

Python is a programming language for general-purpose use released in 1991. It is one of the most popular programming languages and mainly used for the graphical user interface (GUI), websites and application. Python has several advantages over Matlab for this project such as it has a simpler syntax and open source. It is desirable that the product of this project (GUI of severe slugging simulation) is license-free since the main objective is for educational purpose. The libraries that are used for GUI features shown on **Table. 1.2**

No.	Techniques	Method	Drawback
1	Increase separator pressure	Increase back pressure	Decrease production capacity up to 50%
2	Add choke valve	Slightly increase back pressure	Careful choking is necessary to avoid production reduction
3	Gas - lift	Injection of gas at the bottom of the riser	Increase frictional pressure loss and possibility for JT cooling
4	Subsca separator	Produce single phase flow	Complex configuration and operation
5	Self - lifting	Add small bypass line parallel to pipeline	Difficulties in practical application

Table 1.1: Severe slugging elimination techniques.

1.5.2 Visual Studio Code

visual studio code is a development environment software for Python programming from Microsoft. It has functionality for editing, analysis, debugging, and visualization capabilities written in python. Basically it's a program that allow the user to write the python script and run them. There are also other development environment available such as Jupyter, IDLE, Spyder, etc which also has its own advantages.

1.5.3 Excel

Excel is software from Microsoft office that allows the user to organize the data using spreadsheets. In this project, the application of excel mainly used to save files of the results from the simulation. Excel allows the users to organize, plot-specific diagram, and calculate the data from the spreadsheet. Excel also includes sort and filter features that are useful for more detailed analysis. To export the data from python to excel, the pandas library is used for data indexing.

No.	Library	Purpose
1	Pandas	Create dataframe and write data from simulation to excel (export)
2	Matplotlib	Create 2D plot from simulation for the GUI
3	Tkinter	Create and add features for the GUI
4	py2exe	Create executable files (.exe) from python script

Table 1.2: Libraries and its purpose for the GUI.

Chapter 2

Basic Theory

2.1 Flow Regime Map

2.1.1 Stratified Flow

Stratified flow occurs when the gas and liquid phase are separated. The geometry and physical measure that will be used in the model are illustrated in **Fig. 2.1**. The geometrical relationship between liquid holdup (H) and height (h) in a circular cross-section of the pipe can be determined using the geometrical relationship of the wet perimeter half-angle (β).

$$H = \frac{1}{\pi}(\beta - \frac{1}{2}sin(2\beta)) \tag{2.1}$$

Re-arranging and using the approximation within error approximately 0.002 rad, the wet perimeter half-angle can be given as [Biberg and Halvorsen (2000)]:

$$\beta = \pi H + \left(\frac{3\pi}{2}\right)(1 - 2H + H^{\frac{1}{3}} - (1 - H)^{\frac{1}{3}}) \tag{2.2}$$

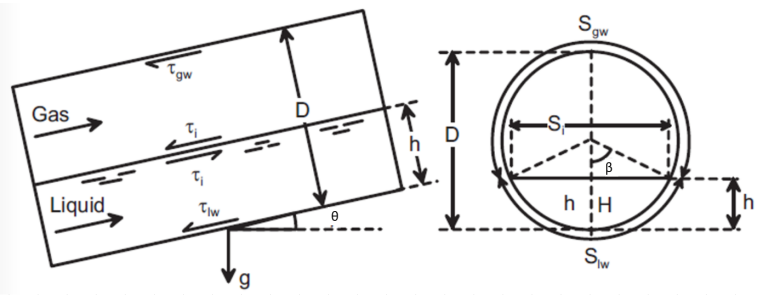

Figure 2.1: Cross sectional geometry for stratified flow [Kristiansen (2004)].

The mass conservation equations in the stratified flow can be written with the assumption for the absence of mass transfer between the phases, droplet entrainment and deposition.

$$\frac{\partial(H\rho_l)}{\partial x} + \frac{1}{A}\frac{\partial(H\rho_l U_l A)}{\partial x} = 0 \tag{2.3}$$

$$\frac{\partial(\alpha\rho_g)}{\partial x} + \frac{1}{A}\frac{\partial(\alpha\rho_g U_g A)}{\partial x} = 0 \tag{2.4}$$

With the assumptions of constant H, equal pressures for liquid and gas phases, as well as ignore the terms for acceleration and convections the momentum conservation equations in the stratified flow can be given. By eliminating both equations, it gives the hold-up equation.

$$-H\frac{\partial p}{\partial x} - \frac{S_{lw}}{A}\tau_{lw} + \frac{S_i}{A}\tau_i + H\rho_l g sin\theta = 0 \tag{2.5}$$

$$-\alpha\frac{\partial p}{\partial x} - \frac{S_{gw}}{A}\tau_{gw} - \frac{S_i}{A}\tau_i + \alpha\rho_g g sin\theta = 0 \tag{2.6}$$

$$\frac{S_i\tau_i}{A} = -H\frac{S_{gw}\tau_{gw}}{A} + \alpha\frac{S_{lw}\tau_{lw}}{A} + H\alpha(sin\theta)(\rho_l - \rho g) \tag{2.7}$$

The friction factors on the wall can be estimated by using Reynolds numbers (Re) that for each phase is given by,

$$Re_g = \frac{U_g\rho_g D_{hg}}{\mu_g} \tag{2.8}$$

$$Re_l = \frac{U_l\rho_g D_{hl}}{\mu_l} \tag{2.9}$$

where the hydraulic diameters for both gas and liquid phases in stratified flow are proposed as follow [Agrawal et al. (1973)]:

$$D_{hg} = 4\frac{A_g}{S_g + S_i} \tag{2.10}$$

$$D_{hl} = 4\frac{A_l}{S_l} \tag{2.11}$$

By using single-phase relations for friction factors, the gas-wall and liquid-wall friction factors (λ) can be estimated for laminar flow and turbulent flow [Kristiansen (2004), Haaland (1983)].

$$\lambda_{tur,g} = \frac{1}{\left[-1.8log_{10}\left(\frac{6.9}{Re_g} + \frac{\varepsilon/D_{hg}}{3.7}\right)^{1.11}\right]^2} \tag{2.12}$$

$$\lambda_{tur,l} = \frac{1}{\left[-1.8log_{10}\left(\frac{6.9}{Re_l} + \frac{\varepsilon/D_{hl}}{3.7}\right)^{1.11}\right]^2} \tag{2.13}$$

$$\lambda_{lam,g} = \frac{64}{Re_g} \tag{2.14}$$

$$\lambda_{lam,l} = \frac{64}{Re_l} \tag{2.15}$$

The final value for the friction factor will be chosen from the highest value between laminar and turbulent flow case. For the interface friction, it often used its relationship with the gas friction factor that neglected the waves [Russell et al. (1974)]

$$\lambda_i = \lambda_g \tag{2.16}$$

For the shear stress τ between gas or liquid and pipe wall or the interface can be estimated by,

$$\tau_i = \frac{\lambda_g}{4} \frac{\rho_g (U_g - Ul)|U_g - Ul|}{2} \tag{2.17}$$

$$\tau_{lw} = \frac{\lambda_l}{4} \frac{\rho_l Ul|Ul|}{2} \tag{2.18}$$

$$\tau_{gw} = \frac{\lambda_g}{4} \frac{\rho_g U_g|U_g|}{2} \tag{2.19}$$

2.1.2 Slug Flow

A unit cell of slug flow consists of different regions, known as a long bubble followed by liquid slug. The part of the slug bubble is considered as a stratified flow where the liquid phase transported at the bottom of the pipe while no droplets entrained in the gas phase. The liquid slug contains the gas bubbles that affected by the buoyancy forces [Kristiansen (2004)]. The geometry and physical measures that will be used in the model are illustrated in **Fig. 2.2**. The continuity across the slug and bubble can be given by [Fuchs (1997)],

$$U_m = U_{sg} + U_{sl} \tag{2.20}$$

$$U_{gs}\alpha_s + U_{ls}(1 - \alpha_s) = U_m \tag{2.21}$$

$$U_{gb}\alpha_b + U_{lb}(1 - \alpha_b) = U_m \tag{2.22}$$

For the liquid phase, the continuity can be given with the assumptions for absences of liquid droplets in the gas bubble and there is no gas mixed into the liquid film, as follows:

$$(1 - \alpha_b)(U_f - U_{lb}) = (1 - \alpha_s)(U_f - U_{ls}) \tag{2.23}$$

$$(1 - \alpha_b)(U_b - U_{lb}) = (1 - \alpha_s)(U_b - U_{ls}) \tag{2.24}$$

The mass balance within the slug unit can be described in terms of the residence time of a slug passing a cross-section of the pipe (t_s) and bubble (t_b) with assumptions of constant α_s, U_{gs} and U_{ls}.

$$U_{sg}(t_s + t_b) = U_{gs}\alpha_s t_s + U_{gb}\alpha_b t_b \tag{2.25}$$

$$U_{sl}(t_s + t_b) = U_{ls}(1 - \alpha_s)t_s + U_{lb}(1 - \alpha_b)t_b \tag{2.26}$$

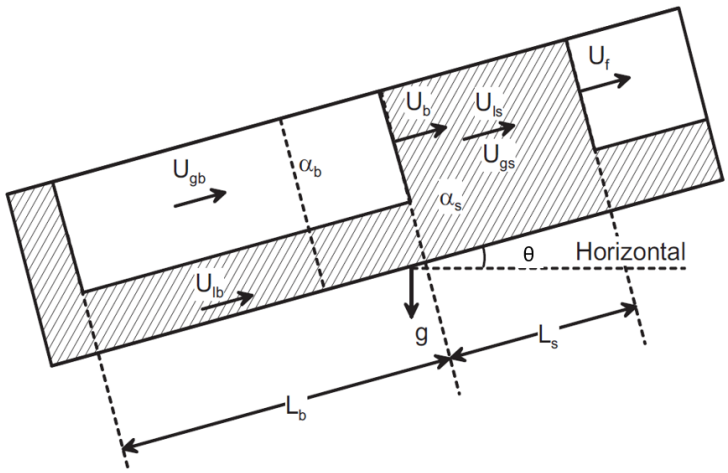

Figure 2.2: Slug unit model that consists of a liquid slug followed by a bubble [Kristiansen (2004)].

where

$$L_s = U_b t_s \tag{2.27}$$

$$L_b = U_b t_b \tag{2.28}$$

The slug fraction (SF) can be determined by using the combined volume balances between slug and bubble fronts.

$$SF = \frac{L_s}{L_s + L_b} \tag{2.29}$$

Re-arranging both equations can give the relation for the slug fraction (SF) as follows:

$$SF = \frac{U_{sl} - U_{lb}(1-\alpha_b)}{U_{ls}(1-\alpha_s) - U_{lb}(1-\alpha_b)} \tag{2.30}$$

A volume balance of liquid hold-up in the bubble and slug sections is used to determine the average liquid hold-up in the slug flow.

$$\alpha = SF\alpha_s + (1-SF)\alpha_b \tag{2.31}$$

The void fraction in the slug (α_s) can be calculated from a universal model that includes surface tension and liquid density by [Malnes (1987)],

$$\alpha_s = \frac{U_m}{83(\frac{g\sigma_{gl}}{\rho_l})^{\frac{1}{4}} + U_m} \tag{2.32}$$

Malnes (1987) suggested that the gas-liquid slip relation as follows:

$$U_{gs} = S_D(U_{ls} + U_{0s}) \tag{2.33}$$

where S_D is the gas-liquid distribution slip in slugs that can be estimated by,

$$S_D = \frac{1 - \alpha_s}{0.95 - \alpha_s} \tag{2.34}$$

U_{0s} is the vertical gas drift velocity in slugs that can be estimated by,

$$U_{0s} = 1.18 \left[\frac{g\sigma_{g/l}(\rho_l - \rho_g)}{\rho_l^2} \right]^{\frac{1}{4}} \sqrt{(1 - \alpha_s)} \tag{2.35}$$

By using the conservation of volume in the slug unit equation, the liquid velocity in slug (U_{ls}) can be calculated once the U_{gs} is substituted and rearranged with U_m.

$$U_{ls} = \frac{U_m - \alpha_s S_D U_{0s}}{(1 - \alpha_s) + \alpha_s S_D} \tag{2.36}$$

Bendiksen (1984) suggested that the bubble front propagation velocity (U_b) can be expressed in terms of superficial mixture velocity (U_m) as follows:

$$U_b = C_0 U_m + U_0 \tag{2.37}$$

where both the C_0 and U_0 value can be determined as a function of the pipe inclination and Froude number (F_r).

$$F_r = \frac{U_m}{\sqrt{\frac{gD(\rho_l - \rho_g)}{\rho_l}}} \tag{2.38}$$

For $F_r > 3.6$

$$C_0 = 1.2 \tag{2.39}$$

$$U_0 = (-0.35 sin\theta) \sqrt{\frac{gD(\rho_l - \rho_g)}{\rho_l}} \tag{2.40}$$

and $F_r < 3.6$

$$C_0 = 1.05 + 0.15 sin^2\theta \tag{2.41}$$

$$U_0 = (-0.35 sin\theta + 0.54 cos\theta) \sqrt{\frac{gD(\rho_l - \rho_g)}{\rho_l}} \tag{2.42}$$

2.1.3 Annular Flow

Annular flow occurs when the gas streams along the center of the pipe while the liquid flows around the pipe walls in the form of a film. The geometry and physical measures that will be used in the model are illustrated in **Fig. 2.3**. For a steady-state in the annular

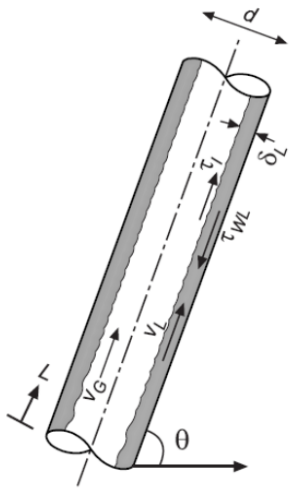

Figure 2.3: Geometry of annular flow with the assumption that there is no entrainment in the gas flows and uniform thickness of liquid's film around the pipe's perimeter [Barnea (1986)].

flow, the momentum or force balance can be determined both in the liquid phase and the gas phase [Alves et al. (1991)].

$$-A_l\frac{dp}{dz} - \tau_{lw}S_{lw} + \tau_i S_i - \rho_l A_l g sin(\theta) = 0 \tag{2.43}$$

$$-A_g\frac{dp}{dz} - \tau_i S_i - \rho_g A_g g sin(\theta) = 0 \tag{2.44}$$

By equating and eliminating the pressure gradient from both equations, the combined momentum equation for annular flow can be derived similar as in stratified flow.

$$\tau_i S_i \left(\frac{1}{A_l} + \frac{1}{A_g}\right) - g(\rho_l - \rho_g)sin(\theta) - \tau_{lw}\frac{S_{lw}}{A_l} = 0 \tag{2.45}$$

The geometry relationships for the film flow can calculated from:

$$S_{lw} = \pi D \tag{2.46}$$

$$S_i = \pi D_g \tag{2.47}$$

where

$$D_g = D\sqrt{\alpha} \tag{2.48}$$

The relation of the shear stress (τ_{lw} and τ_{i}) can be given as,

$$\tau_{lw} = \lambda_l \frac{\rho_l U_l^2}{2} \tag{2.49}$$

$$\tau_i = \lambda_i \frac{\rho_g U_g^2}{2} \tag{2.50}$$

The gas-wall and liquid-wall friction factors (λ) can be estimated for laminar flow and turbulent flow using Wallis's correlation [Barnea (1986)].

$$\lambda_{tur,g} = 0.046\,(Re_g)^{0.2} \tag{2.51}$$

$$\lambda_{tur,l} = 0.046\,(Re_l)^{0.2} \tag{2.52}$$

$$\lambda_{lam,g} = 16\,(Re_g)^{1.0} \tag{2.53}$$

$$\lambda_{lam,l} = 16\,(Re_l)^{1.0} \tag{2.54}$$

Wallis proposed the interface friction can be determined by,

$$\lambda_i = \lambda_g(1 + 150(1 - \sqrt{\alpha})) \tag{2.55}$$

2.2 Regime Transition Criteria

2.2.1 Stratified Stability

One of the theories that can be applied for the stratified stability analysis is a simplified Kelvin-Helmholtz. In general, the instability occurs between two layers of fluid with different densities and flowing with two different velocities in horizontal parallel flat plates. It could predict whether a small disturbance on the surface will lead to a stable or unstable interface [Milne-Thomson (1996)]. Based on this analysis, it explained that the gravity and surface tension forces tend to stabilize the flow while the relative motion of the two layers produces a suction pressure force over the wave from the Bernoulli equation, which tends to create instability for stratified flow. Thus, this theory is further developed a stability criterion in terms of the propagation velocity of the waves and the wavelength [Shoham (2005)]. Once the suction force is greater than the gravity force, the wave growth can occur and lead to an unstable stratified structure. The simplified equation for this transition boundary can be determined as,

$$U_g \geq \left(1 - \frac{h_l}{d}\right)\left[\frac{(\rho_l - \rho_g)gcos(\theta)A_l}{\rho_g S_i}\right]^{0.5} \tag{2.56}$$

the Bernoulli suction force is able to overcome the gravity force if the gas velocity (left-hand side) is higher than the right-hand side expression, causing the unstable flow and thus the transition from stratified into non-stratified flow occurs.

2.2.2 Slug Stability

The stability of the slug flow can be described by investigating the transition to a stratified flow from the slug flow region [Kristiansen (2004)]. Other studies using the slug stability in terms of the criterion where the slug front should propagate with a velocity equal or higher than the bubble front (U_f=U_b) [Bendiksen and Espedal (1992)]. The criterion for slug stability can be expressed by,

$$U_b = \frac{U_{sg} - \alpha_s U_{gs}}{\alpha_b - \alpha_s} \tag{2.57}$$

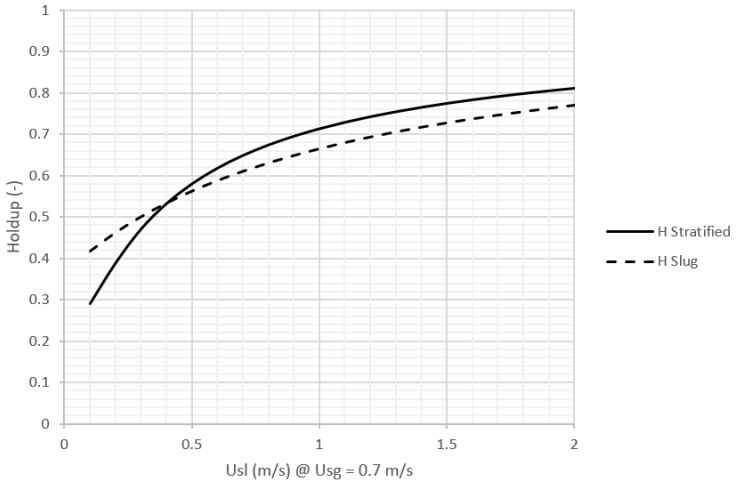

Figure 2.4: Holdup equation from stratified flow model and slug flow model at constant U_{sg}.

where

$$SF = 1 - \frac{U_{sg} - U_{gs}\alpha_s}{U_b(\alpha_b - \alpha_s)} \tag{2.58}$$

During the transition between the slug and stratified flow,

$$S_f = 0 \tag{2.59}$$

The transition of the flow pattern occurs when the slug fraction equals to zero at the point of hold-up continuity (SF $= 0$). In practice, the transition point can be determined by crossing lines between hold up lines from the stratified model and hold up lines from the slug flow model shown in **Fig. 2.4**. For example, from the figure, it can be concluded that the minimum holdup for slug flow occurs at U_{sl}=0.4. Therefore for this case, the transition velocity between stratified and slug flow occur at U_{sl}=0.4 and U_{sg}=0.7.

2.2.3 Annular Stability

Blocking of the gas phase by the liquid waves can promote a transition from annular flow into a slug flow. This condition can result due to two different mechanisms:

- Instability of annular flow
- Spontaneous blockage due to axial transfer of liquid in the film when the wave growth on the liquid film.

Both instability criterion, as well as the spontaneous blockage criterion should be solved simultaneously to determine the transition. The dimensionless film thickness (δ) can achieved from the void fraction.

$$\delta = \frac{1}{2}\left(1 - \sqrt{\alpha}\right) \tag{2.60}$$

Substituting to annular holdup equation becomes,

$$Z = g(\rho_l - \rho_g)Dsin(\theta) \tag{2.61}$$

$$Y = C_l \rho_l \left(Re_l\right)^{-n} \left(U_{sl}\right)^{2-n} \tag{2.62}$$

$$\tau_i = Z(1-2\delta)(\delta - \delta^2) - \frac{1}{32} Y \left[\frac{(1-2\delta)}{(\delta-\delta^2)^2}\right] \tag{2.63}$$

For the first mechanism, the instability occurs when the film is flown backward thus the liquid accumulates cause blockage of the gas in the core, resulting in a transition into slug flow. The instability can be determined at the locus of minimum points which can be calculated by differentiating **Eq. 2.63** and equating it to zero to find minimum film thickness (δ_{min}) as shown in **Fig. 2.5** . The differential equation result as follows:

$$Z\left[(1-2\delta)^2 - 2(\delta-\delta^2)\right] - \frac{1}{16} Y \left[\frac{(\delta-\delta^2) + (1-2\delta)^2}{(\delta-\delta^2)^3}\right] = 0 \tag{2.64}$$

The film minimum thickness can be obtained for a certain value of U_{sg} and U_{sl} which considered as the transition velocity. The second mechanism is the spontaneous blockage that can occur when the liquid flow rates are relatively high, resulting in a thick liquid film that is enough to make the wave growth. In this case, the transition to a slug flow may result from the blockage of the gas phase due to a formation of a liquid bridge across the pipe cross-sectional area that is caused by the large wave. The transition to slug flow will develop at a certain value of α [Barnea (1986)].

$$\alpha < 0.76 \tag{2.65}$$

However, there are limitations to instability criterion. **Fig. 2.5** shows the relationship between the minimum of the curves, corresponding to several inclinations. From the figure, it can be seen that it is not possible to find the minimum point in the horizontal and downward pipeline. Therefore, only the spontaneous blockage mechanisms can occur in downward inclinations.

2.2.4 Dispersed-Bubble Flow

Several studies proposed different mechanisms for the transition boundary to dispersed-bubble flow for different types of flow in horizontal flow and vertical flow. The unified model combines mechanisms that suitable for a wide range of inclination angles. Barnea (1986) suggested that the transition occurs due to two mechanisms:

1. Bubble agglomeration
2. Migration of bubbles to the upper part of the pipe (creaming).

For transition due to bubble agglomeration mechanism, Taitel et al. (1980) and Barnea et al. (1982) proposed that the transition to dispersed-bubble flow may happen in the continuous liquid phase once the turbulent forces overcome surface tension forces to disperse

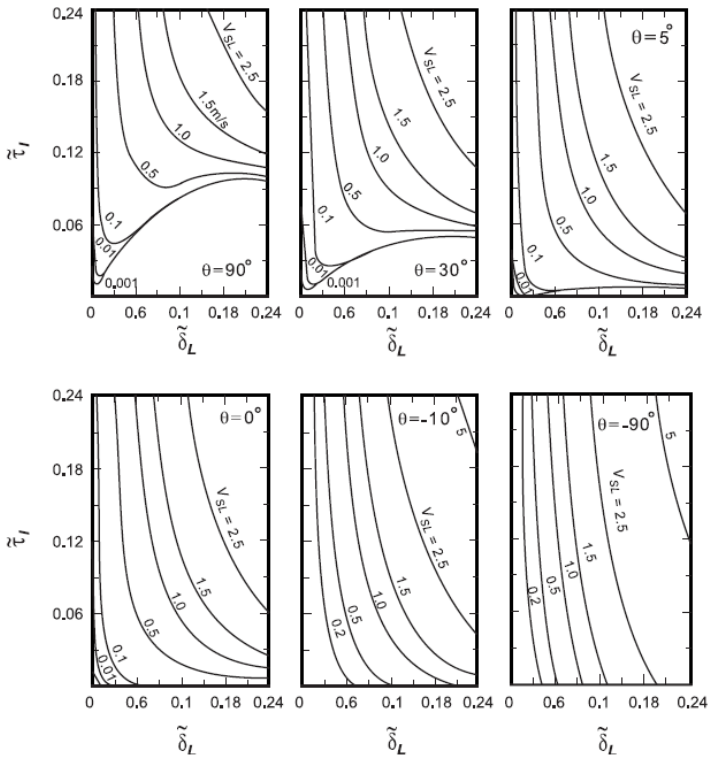

Figure 2.5: Relationships between dimensionless interfacial shear stress (τ_i) and dimensionless film thickness with different inclination angle (δ) [Barnea (1986)].

the gas phase into small bubbles. Based on several studies, the relation for the maximum stable diameter of the dispersed bubbles can be determined as follows [Hinze (1955); Calderbank (1959); Barnea (1986)]:

$$d_{max} = (0.725 + 4.15\sqrt{\alpha})(\sigma/\rho_L)^{0.6}(\varepsilon)^{-0.4} \tag{2.66}$$

where ε for turbulent pipe flow can be given by,

$$\varepsilon = \frac{2\lambda_m}{D}U_m^3 \tag{2.67}$$

This equation is only applied to the dispersed bubble regime when the size of the bubble is small and it prevents agglomeration. However, when the bubble's size is large enough to cause distortion, the agglomeration may be enhanced and the transition from the dispersed-bubble flow may occur. In this condition, the critical size of the bubble (d_{CD}) can be estimated as [Barnea et al. (1982)]:

$$d_{CD} = 2\left[\frac{0.4\sigma}{(\rho_l - \rho_g)g}\right]^{0.5} \tag{2.68}$$

Thus, the transition boundary from the dispersed-bubble can be yielded when the d_{max} is substituted with d_{CD}. In other meanings, the dispersed-bubble flow occurs when the turbulent forces can break the bubbles into small bubbles with a diameter less than the critical diameter [(Shoham, 2005)].

$$d_{MAX} \leq d_{CD} \tag{2.69}$$

The transition due to bubble creaming occurs as when the turbulent forces overcome the buoyancy forces, dispersing the bubbles, and thus promote the dispersed-bubble flow. Oppositely, the buoyancy forces cause the bubbles to be lifted and concentrated in the upper part of the pipe (creaming), which leads to the transition to slug flow. This condition is illustrated in **Fig. 2.6**. The unified model for the bubble creaming's mechanism analysis

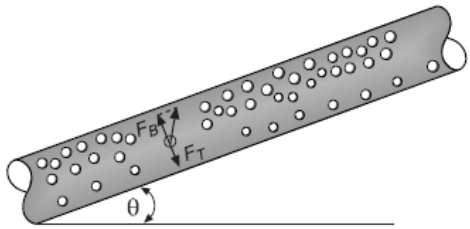

Figure 2.6: Illustration of forces that applied in the dispersed-bubble flow on a single bubble in an inclined pipe with angle θ: buoyancy force (F_B) and turbulent force (F_T).

is performed on a single bubble with diameter of d_B and this mechanism occurs when the critical bubble size (d_{CB}) is large enough to cause creaming. This critical bubble size value can be estimated using the balance between the turbulent and buoyancy forces that can be given as [Shoham (2005); Barnea (1986); Levich (1962)]:

$$F_B = (\rho_l - \rho_g) g cos\theta \frac{\pi d_B^3}{6} \tag{2.70}$$

$$F_T = \frac{1}{2}\, \rho_l U'^2 \frac{\pi d_B^2}{4} \tag{2.71}$$

where the U$^{'}$ can be estimated:

$$(\bar{U'^2}) \approx U^* = U_m \left(\frac{\lambda_m}{2} \right)^{0.5} \tag{2.72}$$

When the buoyancy force is higher than the turbulent force, the transition to the slug flow may occur and the critical bubble diameter for this transition can be estimated and the final criterion for this transition is given by,

$$d_{CB} = \frac{3}{8} \frac{\rho_l}{(\rho_l - \rho_g)} \frac{\lambda_m U_m^2}{g cos\theta} \tag{2.73}$$

$$d_{MAX} \leq d_{CB} \tag{2.74}$$

2.3 Severe Slugging Model

Simplified mathematical models are formulated to simulate severe slugging in L shape riser. Several important parameters such as pressure, friction, hold up, velocity, etc. are calculated for stability criteria. This parameter is determined as an averaged value at the base of the riser. The geometry and physical measures that will be used in the model are illustrated in **Fig. 2.7**. The performance of the model has been verified from experimental data on air-water in s-riser [Martins da Silva et al. (2010)]. The assumptions that used for the model are:

- Isothermal pipeline-riser system
- Ideal gas
- Incompressible liquid
- Gas-liquid interaction is neglected.

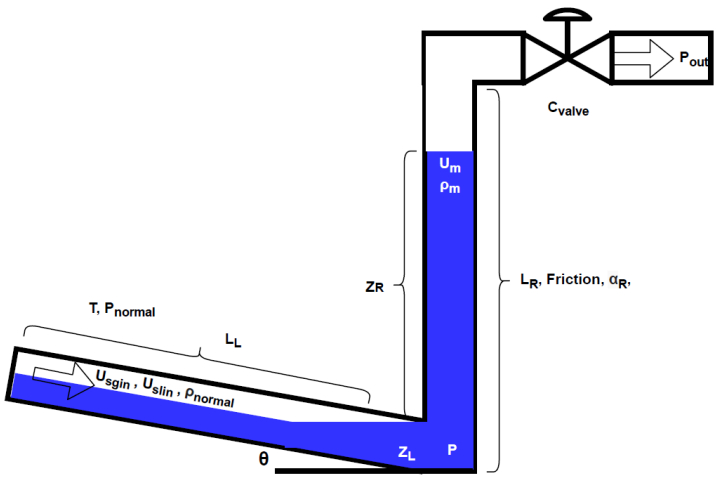

Figure 2.7: Severe slugging modelling variable.

2.3.1 Mass Balance for Riser

The pressure at the base of the riser can be determined using mass balance for the gas phase.

$$\frac{dM_{gL}}{dt} = \frac{d\rho_{gL} L_L A}{dt} = G_{gL} - G_{gR} \tag{2.75}$$

Assuming isothermal, R' is a specific gas constant at a specified temperature (T) and molecular weight (MW).

$$R' = \frac{RT}{MW} \tag{2.76}$$

Using an ideal gas assumption, the relationship between density and pressure can be determined,

$$P = R'\rho \tag{2.77}$$

The mass fluxes can be converted into pressure equation and the inlet flux is specified using pressure at normal condition. The mass flux for the riser section has an unknown variable (U_{sgL}). It will be determined based on three state equation.

$$G_{gL} = AU_{sgin}\rho_{normal} = AU_{sgin}\frac{P_{normal}}{R'} \tag{2.78}$$

$$G_{gR} = U_{sgL}A\rho_g = U_{sgL}A\frac{P}{R'} \tag{2.79}$$

The hold up in the line (L_L) can be computed from the stratified flow model. However, for considerably long pipeline cases the change of (L_L) due to liquid penetrating is small and can be neglected. The pressure equation based on mass balance at the riser becomes,

$$L_L\frac{dP}{dt} = U_{sgin}P_{normal} - U_{sgL}P \tag{2.80}$$

2.3.2 Momentum Balance for Riser

The mixture velocity (U_m) in the riser can be determined using a mixture model for momentum balance. By neglecting interaction between gas and liquid (F_i), only mixture gravity and wall friction that affect mixture velocities.

$$\frac{dL_sA\rho_mU_m}{dt} = A(P - P_{out}) - \tau SL_s - (Gravity)A - \psi A \tag{2.81}$$

The friction term can be calculated by the shear stress between mixture phase and wall. The additional friction such as choke valve and stagnant friction is also included and explained in later section.

$$\tau SL_s = \frac{1}{2}\lambda\rho_L U_m^2 A\frac{z_R}{D} \tag{2.82}$$

The friction factor for the mixture phase are calculated using Haaland's equation mentioned in **Eq. 2.12**. The gravity term is determined from the pipeline liquid level (z_L) and riser mixture level (z_R). The density for the riser is calculated as a mixture phase (bubbly flow) while for the pipeline as liquid phase (stratified flow).

$$(Gravity) = -\rho_l g z_L \sin(\theta) + \rho_m g z_R \tag{2.83}$$

The mixture level for the riser can be determined from the holdup.

$$z_R = -z_L + (1 - \alpha_R)L_R \tag{2.84}$$

while the liquid level in the pipeline can be calculated from integrating the change between mixture velocity in riser and liquid velocity in the pipeline. Some limitations are applied to avoid the flow back to the pipeline from the riser. Therefore, the following equation is applied for $z_L < 0$ or $z_L = 0$.

$$\frac{dz_L}{dt} = U_m - U_{slin} \tag{2.85}$$

The length of the slug is calculated by considering level and mixture density. The mixture density is calculated using the holdup.

$$L_s\rho_m = -z_L\rho_l + L_R\rho_m \tag{2.86}$$

$$\rho_m = \alpha_R\rho_{gR} + (1 - \alpha_R)\rho_l \tag{2.87}$$

2.3.3 Holdup Equation

The phase fraction for both pipeline and riser can be determined using the volume balance. There are 4 new variables (U_{sgL}, U_{sgR}, U_{slL}, U_{slR}) that can determined using three state equation.

$$\frac{dL_R\alpha_R}{dt} = U_{sgL} - U_{sgR} \tag{2.88}$$

$$\frac{dL_R(1 - \alpha_R)}{dt} = U_{slL} - U_{slR} \tag{2.89}$$

Assuming incompressible flow, the holdup equation in the riser becomes,

$$2\frac{dL_R\alpha_R}{dt} = U_{sgL} - U_{sgR} - U_{slL} + U_{slR} \tag{2.90}$$

2.3.4 Three State Equation

The three-state describe on **Table. 2.1** and illustrated in **Fig. 2.8**. The first state is the blowout which can be determined by positive U_m and z_L. During the blowout, the gas is penetrated through the riser. The pressure at the bottom of the riser will decrease and U_m spike during the blowout. The equation for the gas velocity during this state is determined using slip relation [Bendiksen et al. (1991)].

$$U_g = 1.2U_m + 0.35(gD)^{0.5} \tag{2.91}$$

The second state is the slug generation determined by positive U_m and negative z_L. During slug generation, the liquid level in the pipeline is increasing due to U_{slin} higher than U_m. At the current condition, the pressure is build up at the base of the riser. The third state is determined by negative U_m and negative z_L. This state is the opposite of the second state where the U_m going back to the pipeline. Therefore the equation is the same for both states.

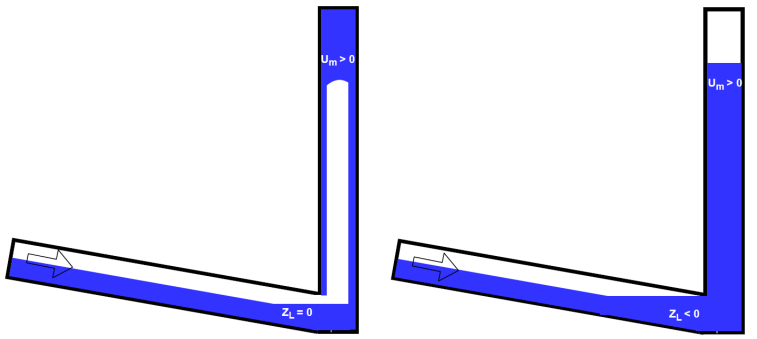

Figure 2.8: Severe slugging three-state model.

State	**U_m**	**z_L**	U_{sgL}	U_{slL}	U_{sgR}	U_{slR}
1	$U_m>0$	$z_L=0$	$U_m - U_{sLin}$	U_{sLin}	$\alpha_R U_g$	$U_m - U_{sgR}$
2	$U_m>0$	$z_L<0$	0	U_m	U_m	0
3	$U_m<0$	$z_L<0$	0	U_m	U_m	0

Table 2.1: Severe slugging three-state equations

2.3.5 Additional Friction

Two additional frictions added for the momentum balance. The first one is friction to damp out z_L oscillation during slug generation (state 2). A new variable is defined as level velocity (U_{level}) for the pipeline which is the difference between U_m and U_{slin}.

$$U_{level} = \frac{dz_L}{dt} = U_m - U_{slin} \tag{2.92}$$

The damping factor can be calculated as a level velocity function for the additional friction terms. K is the damping factor which in this case, the value 10 is enough to reduce the z_L oscillation but still give negligible value to affect momentum balance during blowout (state 1).

$$\psi_1 = \frac{1}{2}(K)\rho_l U_{level}^2 \frac{z_R}{D} \tag{2.93}$$

Choking was found to be able to eliminate severe slugging by acting through backpressure. Choking can also increase the cycle time by reducing blowout velocity from the riser [Jansen et al. (1996)]. The additional friction from choke could make the system more stable to an acceptable level of oscillation until almost no oscillation. Choking can be implemented to momentum balance as an additional friction term. Choking can be formulated as a mixture velocity function by implementing a simple choke valve equation.

$$w_{out} = C_v f \sqrt{\rho P_{drop}} \tag{2.94}$$

while C_v and f are valve constant and opening, respectively. The simple choke equation as an additional friction term for momentum balance can be computed.

$$\psi_2 = C_{valve} U_m^2 \rho_L \tag{2.95}$$

while C_{valve} could have specific value determined from type of valve, cross section and opening for multiphase flow case.

Chapter 3

Methodology

3.1 Numerical Method

In general, two main problems need to be solved: severe slugging stability map and flow regime map. Both of the models need different approaches therefore they also need to be solved separately.

3.1.1 Numerical Integration

The numerical integration is necessary to solve the differential equation in the severe slugging model. Euler's method is implemented for numerical integration to solve the first-order differential equation. Therefore the slug initiation based on full liquid at the riser is necessary to start the model. The initial values for several parameters are tabulated in **Table. 3.1** The results are then stored for each step (i) with total n steps. The equations that need to be solved using this method are the pressure equation (mass balance), flow equation (momentum balance), holdup equation (volume balance), and liquid level equation.

Parameter	Initial Value	Unit	Note
ρ_{gR}	1	kg/m^3	
ρ_m	1000	kg/m^3	Full liquid in the riser
α_R	0	-	Full liquid in the riser
P	261865	Pa	Full liquid in the riser
z_L	0	m	
U_{Level}	0	m/s	
ρ_{gL}	2.6	kg/m^3	From P/R*
$U_{sgboundary}$	1	m/s	Transition from $U_{sg} > 1$ m/s

Table 3.1: Initial values for numerical calculations.

$$P_{(i+1)} = P_{(i)} + \frac{\Delta t}{L_L}(U_{sgin}P_{normal} - U_{sgL(i)}P_{(i)}) \tag{3.1}$$

$$U_{m(i+1)} = \frac{\Delta t}{(L_s\rho_m)_{(i)}}((P_{(i)} - P_{out}) - \frac{(\tau SL_s)_{(i)}}{A} - (Gravity)_{(i)} - \psi_{(i)}) + U_{m(i)} \tag{3.2}$$

$$\alpha_{R(i+1)} = \frac{\Delta t}{2L_R}(U_{sgL(i)} - U_{sgR(i)} - U_{slL(i)} + U_{slR(i)}) + \alpha_{R(i)} \tag{3.3}$$

$$z_{L(i+1)} = \Delta t(U_m - U_{slin}) + z_{L(i)} \tag{3.4}$$

$$\Delta t = \frac{time}{N_{step}} \tag{3.5}$$

3.1.2 Boolean Function

The boolean function is implemented to solve the three-state model. The function value is based on the given statement. The value for true is 1 and the value for false is 0. The function is useful for a certain case such as three state equations and friction model based on the Reynolds number.

$$\delta(True) = 1 \tag{3.6}$$
$$\delta(False) = 0 \tag{3.7}$$

$$U_{sgL} = (U_m - U_{slin})\delta(U_m > 0)\delta(z_L > 0) \tag{3.8}$$

$$U_{slL} = (U_{slin}\delta(z_L > 0) + U_m\delta(z_L < 0))\delta(U_m > 0) + U_m\delta(U_m < 0) \tag{3.9}$$

$$U_{sgR} = (\alpha_R U_g\delta(z_L > 0) + U_m\delta(z_L < 0))\delta(U_m > 0) + U_m\delta(U_m < 0) \tag{3.10}$$

$$U_{slR} = (U_m - \alpha_R U_g)\delta(U_m > 0)\delta(z_L > 0) \tag{3.11}$$

3.1.3 Bisection method

The bisection method is a known numerical method used to find root from continuous function. For severe slugging stability map application, the bisection method used to find the U_{sg} inlet boundary (root) from stability function (continuous function). The iteration begins with one U_{sl} inlet and two initial values of U_{sg} inlet (U_{sg} inlet a and U_{sg} inlet b) that give two opposite signs for the output of the function. For the flow regime map application, the bisection method used to find void fraction (α) of stratified, slug, and bubble flow as the root. The iteration is illustrated on **Fig. 3.1** [Mathews et al. (2004)].

$$a = U_{sgin} \tag{3.12}$$

$$b = U_{sgin} + U_{steps} \tag{3.13}$$

In the next step, a new input value can be defined from the middle point between a and b. If the input c gives positive results then c will be the new a and if negative c will be the new b. The iteration will continue until $f_{stability}(c)$ gives the value near zero then c can be defined as the U_{sg} inlet boundary. The results of this method are a series of data of U_{sl} inlet versus U_{sg} inlet at slug boundary condition.

$$c = \frac{a+b}{2} \tag{3.14}$$

$$a = c * (f_{stability}(c) > 0) \tag{3.15}$$

$$b = c * (f_{stability}(c) < 0) \tag{3.16}$$

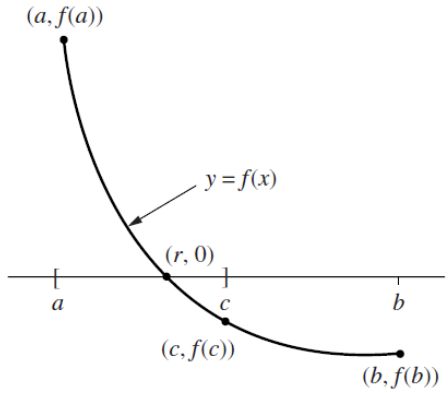

Figure 3.1: Illustration of bisection method.

3.2 User's Input

In this section, the initial value and user's input for the GUI are described. The data for the user's input default value is tabulated on **Table. 3.2**. Both the flow regime maps and the severe slugging model shared the same input.

3.3 Algorithms

In this section, the algorithms for the numerical calculations are described. In general, it consists of the algorithms for the severe slugging stability map and flows regime map. Both of them involves bisection method algorithm with purpose to find the exact value of U_{sg} and U_{sl} that the transition will occur.

Parameter	Default Value	Unit
ρ_l	900	kg/m^3
ρ_g	5	kg/m^3
μ_l	0.001	Pa.s
μ_g	0.0001	Pa.s
R*	100000	J/kg
D	0.05	m
Surface tension	0.05	J/kg
Roughness	0.0000025	m
L_L	200	m
L_R	15	m
Angle (θ)	-5	-
P_{normal}	100000	Pa
P_{out}	100000	Pa
U_{sgmin}	0	m/s
U_{sgmax}	50	m/s
C_{valve}	0	-
N_{step}	100	-

Table 3.2: GUI user's input.

3.3.1 Severe Slugging Stability Map

The first step of the algorithm for severe slugging stability map shown in **Fig. 3.2**. For each iteration, the results of pressure at the bottom of the riser (P_{riser}) will be stored as a list for the stability calculation. The second step is to analyze the results for each combination of U_{sg} and U_{sl} of the severe slugging unit. The overall algorithm for the slug stability map is shown in **Fig.3.3**. To achieve the result, the calculation is programmed to solve the severe slugging model for each combination of U_{sg} and U_{sl}. Therefore, the bisection method is used to find the exact value of U_{sg} and U_{sl} that can determine stable-unstable criteria. The algorithm for the bisection method is shown in **Fig.3.4**.

3.3.2 Flow Regime Map

For the flow regime map, the main iteration to find a combination of U_{sg} and U_{sl} is identical. The difference can be found for each transition model that has unique transition criteria such as a dispersed bubble. The first step of the algorithm begins with the holdup equation either for the slug, annular, or stratified flow using the bisection method shown in **Fig. 3.5**. In this case, the method is used to find void fraction (α) at certain combination of U_{sg} and U_{sl}. The second step is to check every combination of user-specified U_{sg} and U_{sl} that the transition will occur. For example, the input is U_{sg} at the range from 0 to 100 m/s and the result will be U_{sl} at transition line within 0 to 10. Both of the algorithms shown in **Fig. 3.6** and **Fig. 3.7**.

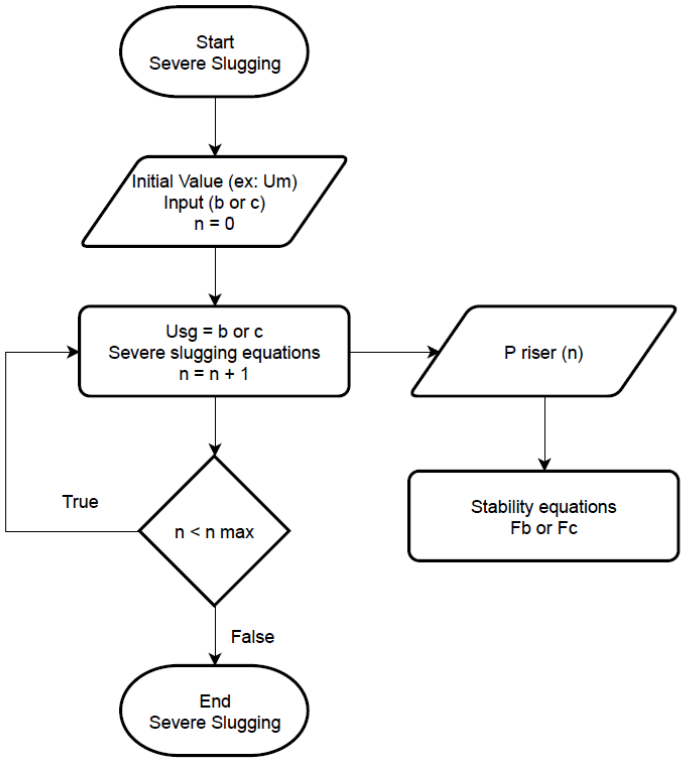

Figure 3.2: A unit of severe slugging iteration for each U_{sg} and U_{sl}.

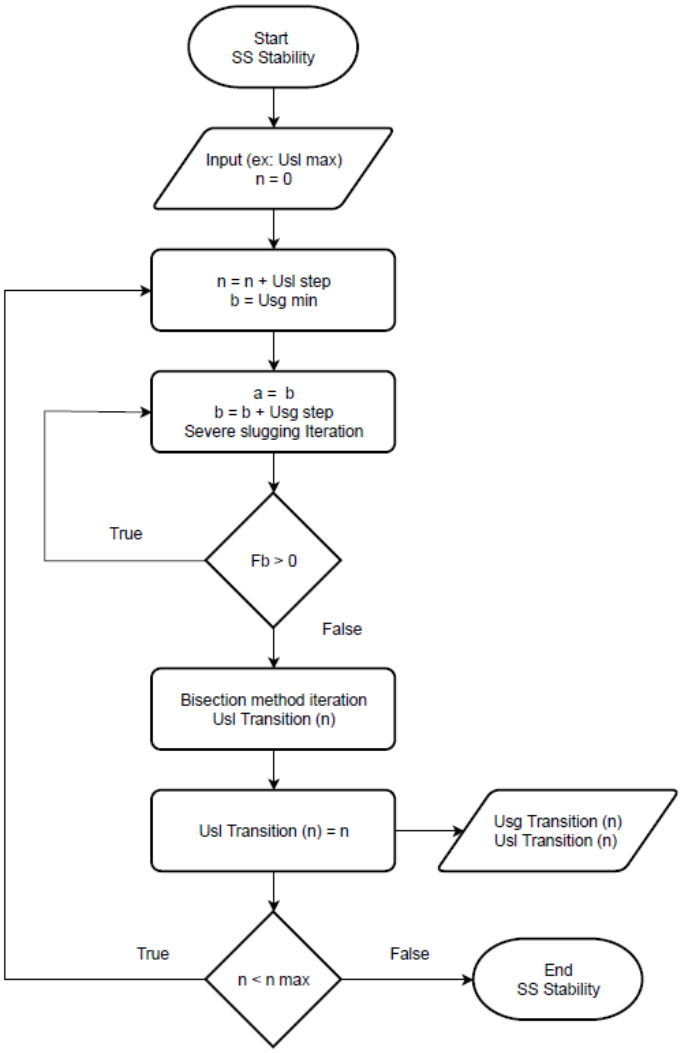

Figure 3.3: Overall iteration to find each of U_{sg} and U_{sl} at stable-unstable transition for severe slugging.

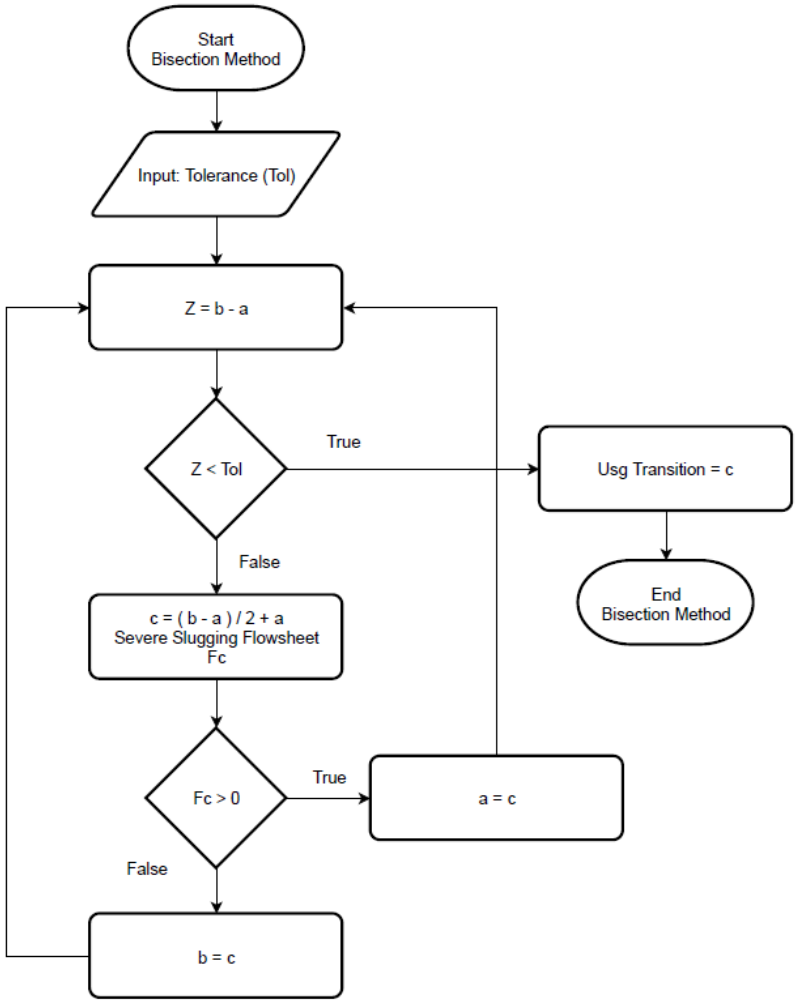

Figure 3.4: Bisection method iteration to find the root (U_{sg}) that will give the value of F near zero.

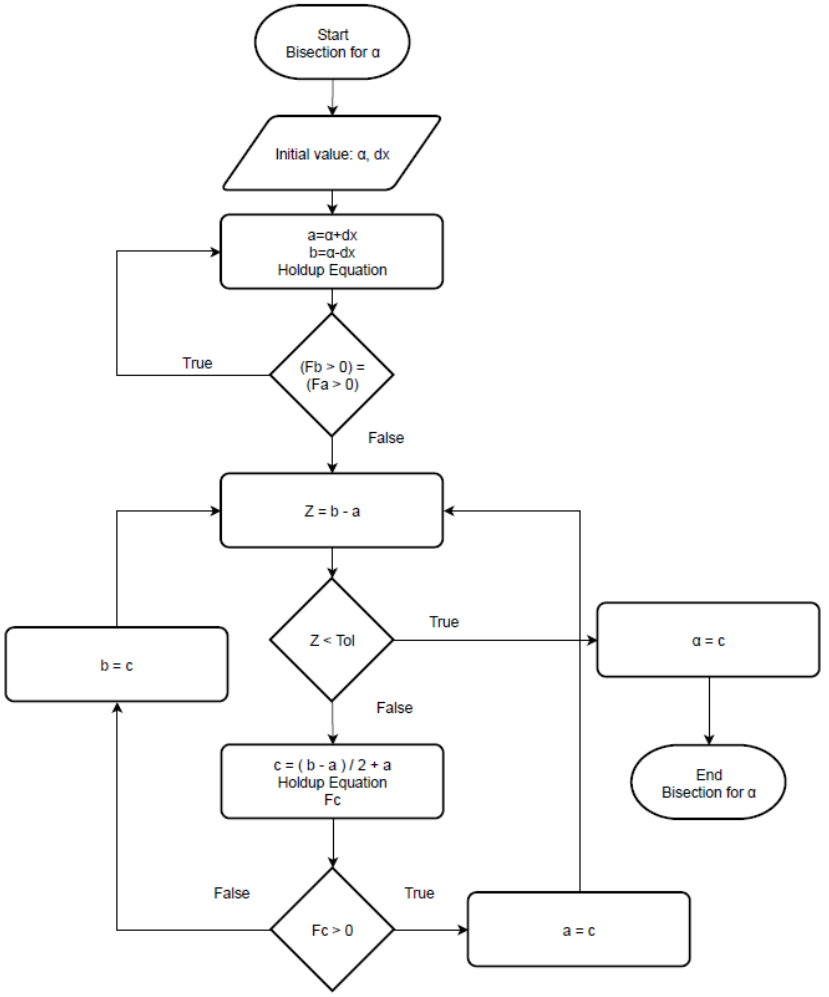

Figure 3.5: Bisection method iteration to find the root (α) that will give the value of error from holdup equation near zero.

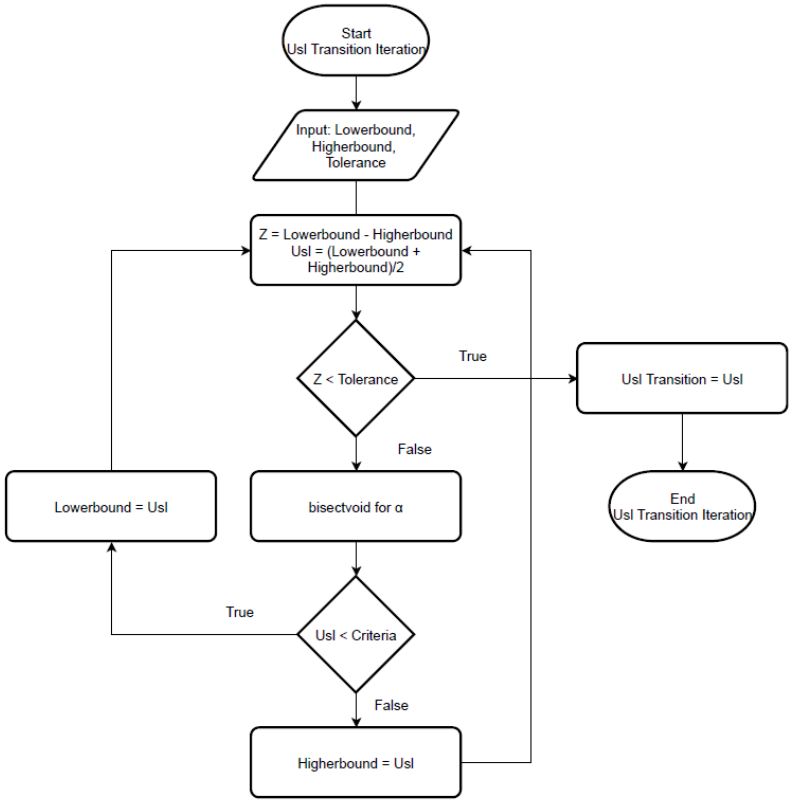

Figure 3.6: Iteration to find U_{sl} based on criteria from selected flow regime for each value of U_{sg}.

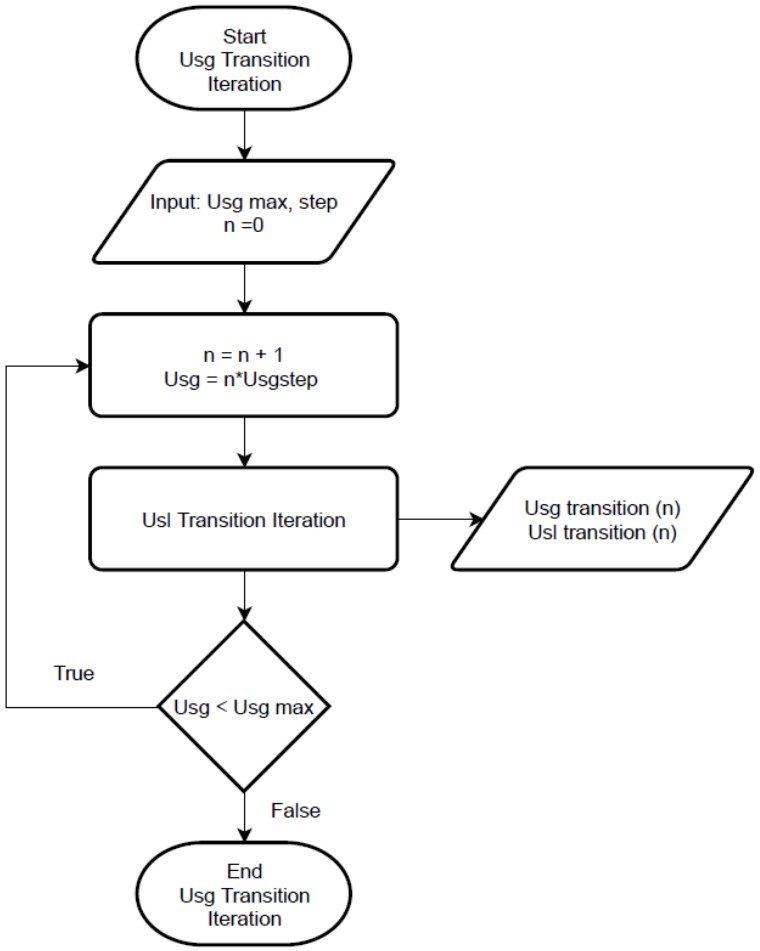

Figure 3.7: Overall iteration to find each of U_{sg} and U_{sl} at selected flow regime transition.

Chapter 4

Discussion and Analysis

In this section, the final design of the Graphical User Interface (GUI), and the result of the flow regime map and severe slugging stability map will be discussed. The sensitivity analysis was conducted for several chosen factors to observe their effect on the flow patterns transition through the flow regime maps.

4.1 Graphical User Interface

The graphical user interface (GUI) for the model is shown in **Fig. 4.1**. The GUI has been made in python using the Tkinter library and the plot using the Matplotlib library. The GUI is divided into two main features that consist of a flow map and a holdup curve. The resulting plot can show the selected transition line from the data storage up to two-curve for each plot. For example, the left-hand side plot is the result of the transition map for severe slugging stability, bubble-dispersed transition, and annular stability. The purpose of this feature is to compare the selected stability curve at a different velocity. The middle and right-hand side plot is a holdup equation for the selected flow regime and velocity. The purpose of the export command is to store the data to an excel file for further analysis.

4.2 Severe Slugging Model

The results of the model show that it can simulate the three-state model of severe slugging for the riser-pipeline system. **Fig. 4.2, Fig. 4.3, Fig. 4.4** shows the result of the pressure (P), mixture velocity in the riser (U_m), and Holdup behaviors in time for specific inlet velocity. The model allows the to distinguish between slug generation, gas compression, and blowout. During slug generation, the liquid accumulates the riser which causes the pressure and holdup increase while the top of the riser does not produce any liquid or gas (U_m = 0). After the holdup is maximum (H=1), the gas continues to compress at the bottom of the riser until it reaches the maximum pressure (1.9 to 2.65 bar). The next stage

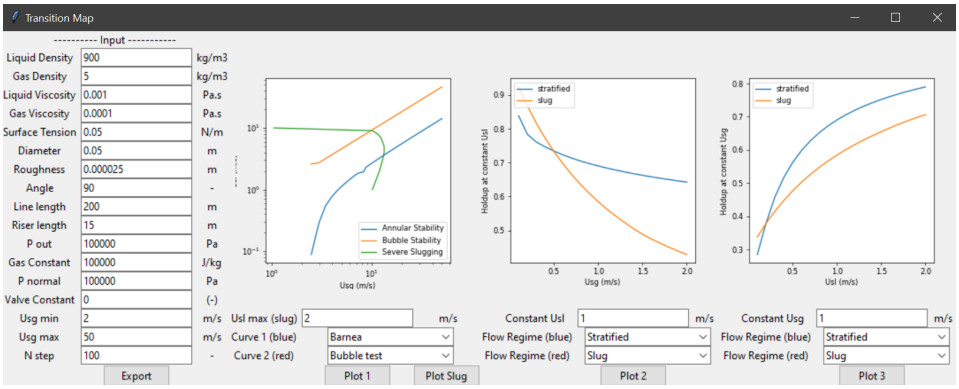

Figure 4.1: Graphical user interface (GUI) result from the model on default value input

is the blowout as the pressure and holdup decrease (1.4 to 1.9 bar increase) followed by an acceleration of the liquid.

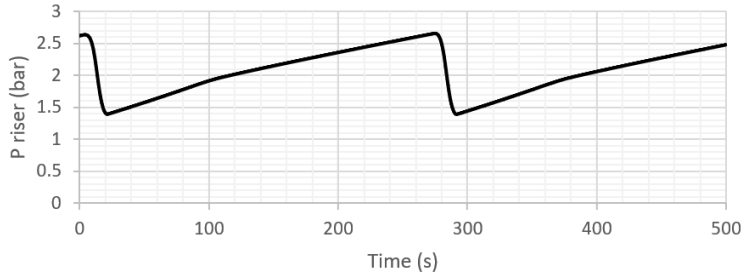

Figure 4.2: Pressure at the bottom of the riser versus time at U_{sg} = 0.5 m/s, U_{sl} = 0.3 m/s

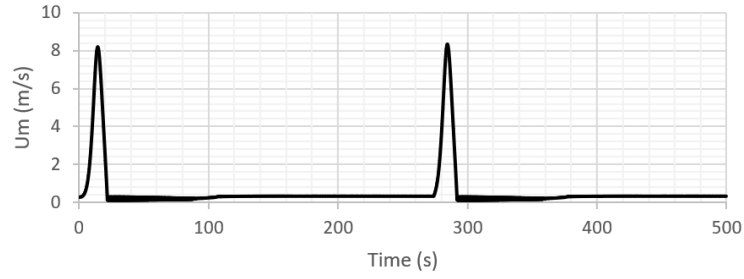

Figure 4.3: Mixture velocity at the riser versus time

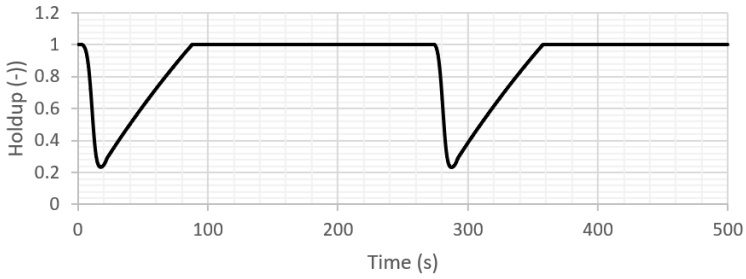

Figure 4.4: Holdup at the riser versus time

4.3 Severe Slugging Stability Criterion

Statistical analysis was formulated to determine severe slugging boundaries. The transition between stable and unstable flow occurred during the increasing of the superficial velocity of the liquid inlet (U_{slin}) to solve the superficial velocity of the gas inlet (U_{sgin}). The series of data of pressure for each time calculated from the severe slugging model was used for this analysis. Response time is necessary to consider to avoid taking transient conditions from severe slugging initiation. Therefore, the data used for this analysis is for half end, by assuming a steady-state has been reached ($P_{half\ end}$). The criteria for stable flow are defined by the value of $F_{stability}$.

$$X = [P_{(n/2)}, P_{(n/2+1)}, ..., P_{(n)}] \tag{4.1}$$

$$F_{stability} = \frac{max(X)}{mean(X)} - 1 \tag{4.2}$$

The result from the stability function will give the value positive for severe slugging, negative for steady-state, and near-zero at boundary condition. Stability tolerance (ST) is defined as a boundary condition between steady-state and severe slugging. In this case, a 10% offset of pressure oscillation is acceptable as a boundary condition shown in Fig. 4.5.

4.4 Flow Regime Maps

The result of the flow regime map that has been developed from the calculation for default value input shown in Fig. 4.6. There are several types of flow regimes that can occur. It may depend on several factors such as flow rate of gas and liquid, the geometry of the pipe (diameter, inclination, and wall wetting), fluid properties (density, viscosity, and surface tension), and the system (pipe length and inlet conditions/flow development). As mention before, the input of the simulation involves fluid properties which could change by pressure oscillation in the system. Therefore sensitivity analysis of density, pipe inclination and viscosity is made.

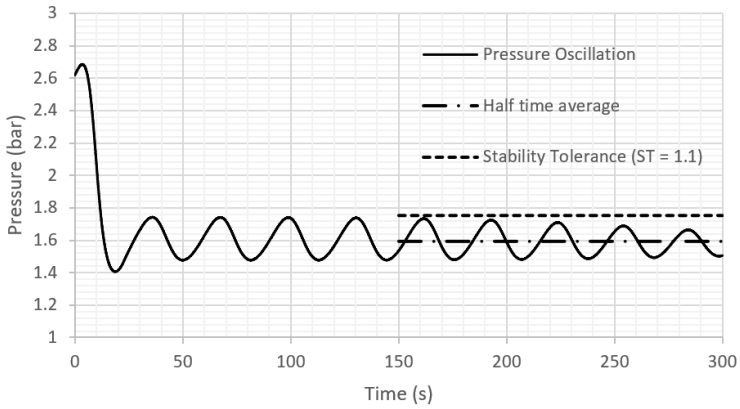

Figure 4.5: Severe slugging stability criterion

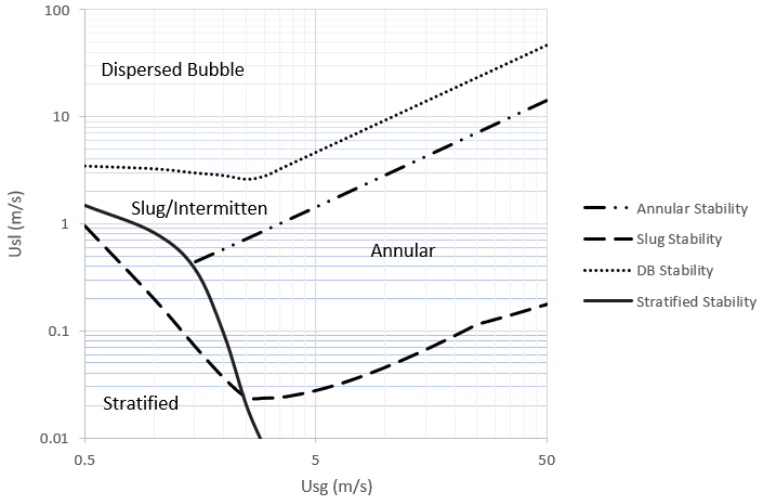

Figure 4.6: Flow regime map result at the default value (**see Chapter. 3**)

4.4.1 Effect of Pipe Inclination

The simulation was conducted to study the effect of pipe inclination on the transition of flow regimes by using two different negative angles. The results are shown in **Fig. 4.7**. The results show that at a higher downward inclination, it is observed that the stratified region is increasing while the slug region is decreasing. This condition may occur as the liquid move faster at the downward inclination, resulting in a lower level of height so that it requires a higher gas and liquid flow rates to obtain and keep the transition from stratified to slug flow. Thus, it is expected that as the pipe is shifted downwards, the slug region is decreasing [Kristiansen (2004)]. The effect of the pipe inclination is large at the lower superficial gas velocity. This observation was agreed with a previous study by

Kristiansen (2004) that the small changes in the pipe inclination may have a large effect on the stratified-slug flow pattern transition, that are only observable at low gas flow rates at which the gravitational effects are dominating. He also stated that for negative pipe angles, there will be an increased tendency towards liquid stratification as the result of the gravity forces that work in the same direction as the flow and it requires a higher liquid flow rate to form slug flow.

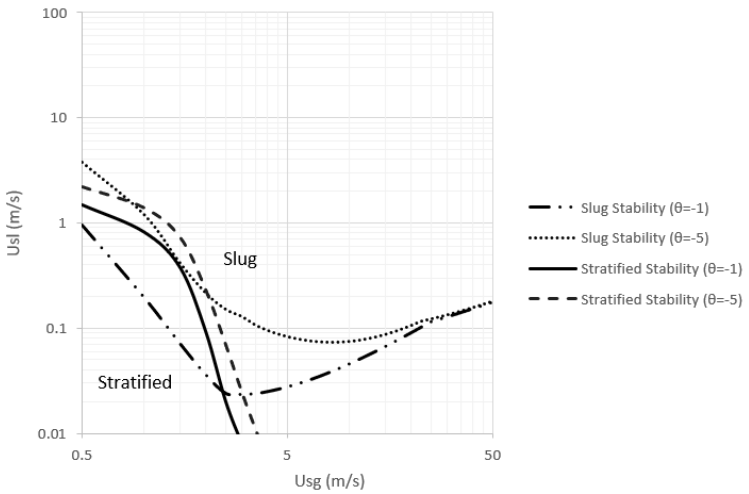

Figure 4.7: The effect of different pipe inclinations on the flow regimes in the pipeline

4.4.2 Effect of Density

The second factor that was chosen to be observed was the changes in different densities of the gas phase, both in the pipeline and the riser case. For the pipeline, the flow regimes were analyzed for stratified and slug flow while for the riser, annular and dispersed bubble flow were observed. Their effects on the flow patterns can be seen in **Fig. 4.8** and **Fig. 4.9**.

The simulation result for changing the gas densities in the pipeline at (=-1) pipe inclination was observed that at the lower gas flow rate, the increase of gas density could decrease the stratified flow region while the slug region remained the same. However, at the higher gas flow rate, the slug region tended to reduce for a higher gas density. This condition is expected as the higher gas density may increase the drag between the gas and liquid phase, resulting in less hold-up in the pipe and thus decrease the tendency to slugging, and this was observed at high pressure.

On the other hand, the simulation for the flow pattern transition in the riser with the same different gas densities showed that the dispersed bubble region remained the same for two different gas densities while the annular flow region tended to increase as the increase of the gas density that can be observed at the higher gas flow rates.

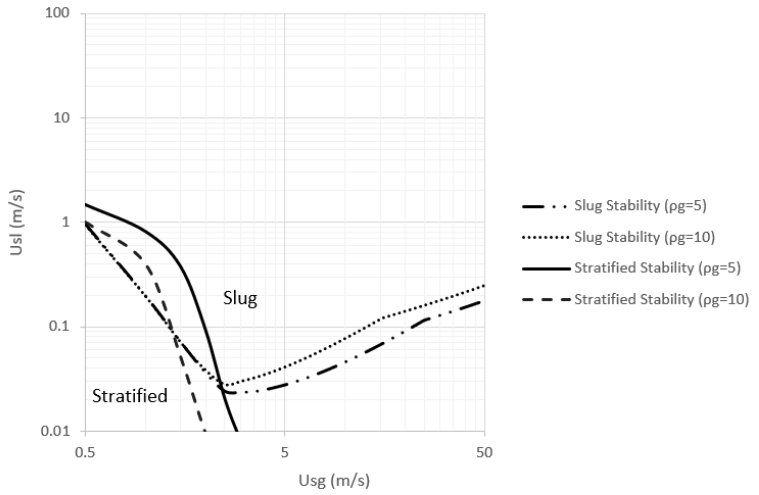

Figure 4.8: The effect of different gas densities on the flow regimes in the pipeline at θ=-1

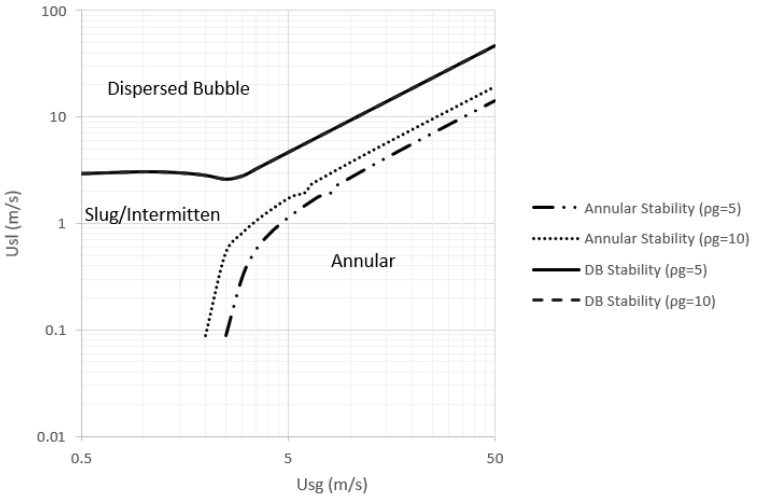

Figure 4.9: The effect of different gas densities on the flow regimes in the riser at θ=90

4.4.3 Effect of Viscosity

The effect of changes in gas viscosity on the flow regime transitions was analyzed by doing the simulations for two different values of gas viscosity in the riser as well as in the pipeline. The results are presented in **Fig. 4.10** and **Fig. 4.11**.

The simulation for the riser showed that the dispersed bubble flow regime did not change for different gas viscosity at any gas flow rate. On the other hand, the effect was observed for the annular regime at higher gas flow rates that the annular region increased at a higher

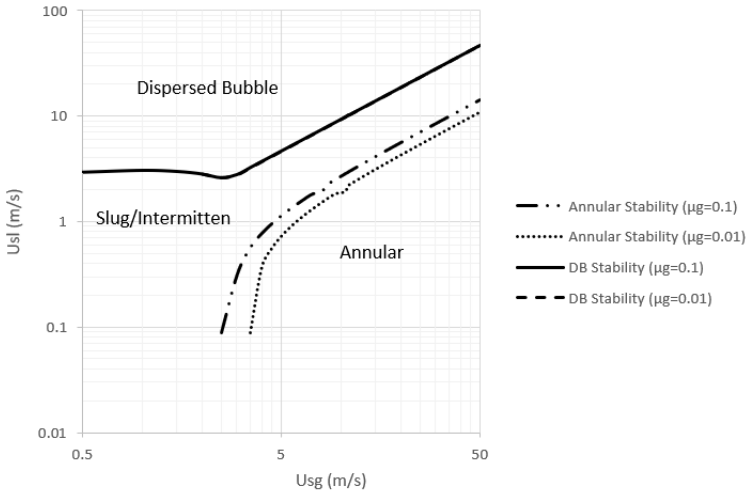

Figure 4.10: The effect of different gas viscosity on the flow regime in the riser at θ=90

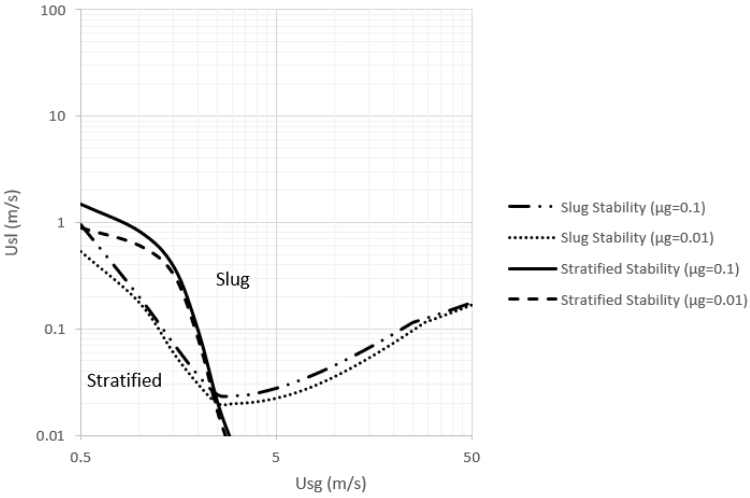

Figure 4.11: The effect of different gas viscosity on the flow regime in the pipeline at θ=-1

gas viscosity. For the pipeline simulation, at the lower gas flow rate, the stratified region rose as the gas viscosity increased. However, the slug region tended to slightly decrease at the higher gas viscosity and lower gas velocity.

The results for the effect of different liquid viscosity are presented in **Fig. 4.12** and **Fig. 4.13** in the riser and pipeline, respectively. In general, the simulations showed the opposite conditions compared to the gas viscosity effect. In the riser, the higher liquid viscosity could slightly decrease the annular flow region at the higher gas flow rate while at the

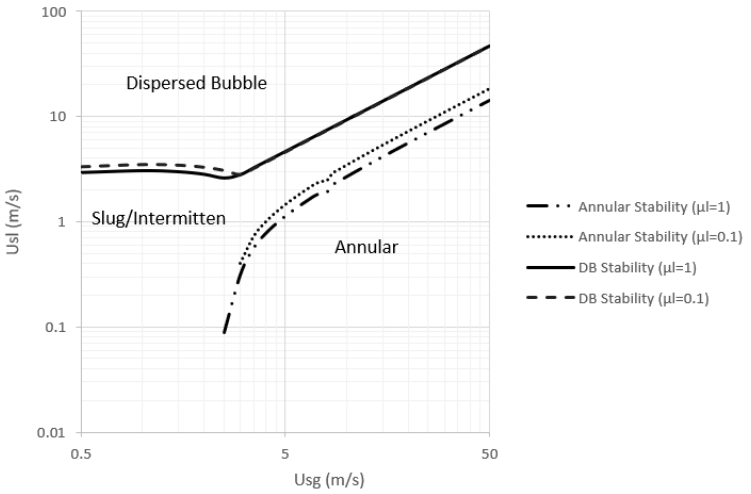

Figure 4.12: The effect of different liquid viscosity on the flow regime in the riser at θ=90

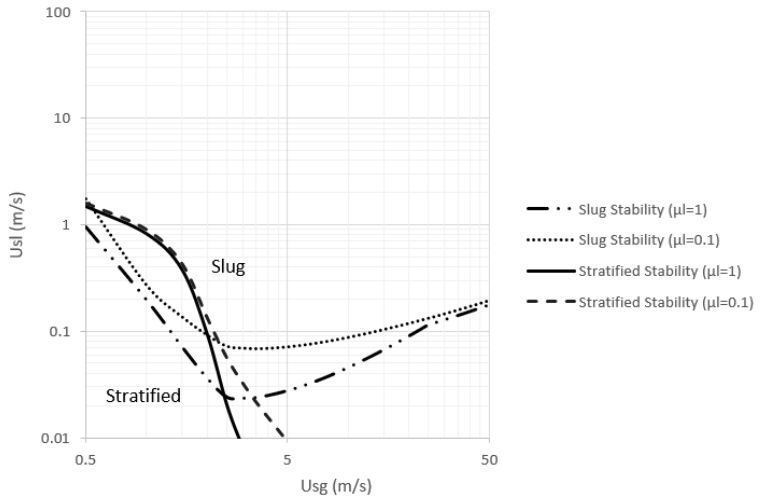

Figure 4.13: The effect of different liquid viscosity on the flow regime in the pipeline at θ=-1

lower gas flow rate, it slightly increase the dispersed bubble region. For the pipeline, the stratified region slowly began to reduce towards the higher gas velocity with the increasing of liquid viscosity but the slug region increased for the higher liquid viscosity.

An increase in the liquid viscosity increases the stability of the interface in stratified flow, causing the transition from stratified flow to slug flow to occur at higher liquid flow rates. The higher critical U_{sl} for high liquid viscosity reflects the increased resistance of the wall to the liquid flow for a given U_{sg}. This indicates that increasing the liquid viscosity also

increases both the liquid wall shear stress and the interface shear stress. Increasing the viscosity have the same effect as reducing the Reynolds number proclaimed in the equation which increases pipe wall friction. For stratified flow, only the liquid friction terms in the holdup equation are affected, yielding a negative effect on the liquid holdup for given conditions.

4.5 Severe Slugging Stability Map

The stability map is conducted to distinguish the regions between severe slugging and steady-state regions. The comparison for the pipeline is presented in **Fig. 4.14**. The area above the left-hand side severe slugging stability line is the unstable region while on the right-hand side is the stable region. It is shown that a partial region of an unstable state is inside the annular flow and dispersed bubble flow regime. In this region, liquid build up in the riser that could lead to severe slugging does not occur. This can be proven by the ability of gas penetration through the riser under annular flow or dispersed bubble.

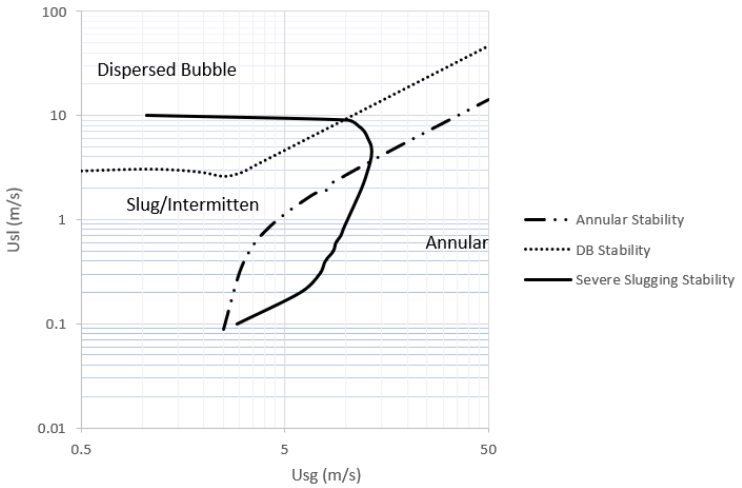

Figure 4.14: Comparison of severe slugging stability map with the flow regime in the riser (θ=90)

The comparison for the pipeline is presented in **Fig. 4.15**. It is shown that a partial region of the unstable state is inside non-stratified flow in the pipeline. In this region, severe slugging type I (slug length equals to the length of the riser) does not occur. To put the system under severe slugging type I, an accumulation of a sufficient amount of liquid at the riser base is necessary to create a full blockage. There is a possibility of severe slugging type II (slug length less than the length of the riser) occurrence under the slug flow region in the pipeline and unstable region. Severe slugging type II is qualitatively have shorter oscillation than type I. During the severe slugging type II, some of the gas penetrated at the riser base which led to smaller pressure oscillation. The model of severe slugging in this work is limited to full blockage at the riser base (type I), therefore it is not possible to

simulate severe slugging type II stability.

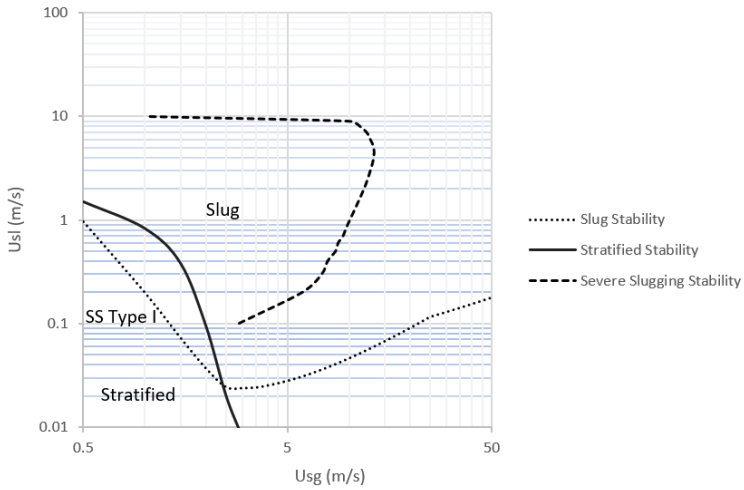

Figure 4.15: Comparison of severe slugging stability map with the flow regime in the pipeline (θ=-1)

Chapter 5

Conclusion

The project aims to design the Graphical User Interface (GUI) in order to generate the severe slugging stability map and sever slugging generating map. Based on the results of the project, several points can be concluded as follows:

1. The simplified mathematical model is able to simulate the severe slugging conditions.
2. Flow transition criteria is able to simulate flow regime map.
3. The Graphical User Interface (GUI) of the selected model has been implemented using Python.
4. The GUI has three main features that consist of results plot, flow regime map and severe slugging transition map.

In the end, the final design of the GUI can be constructed for the simple flow line-riser system that is useful to avoid an operational problem caused by severe slugging. However, there is always a limitation in the design such as the fluid properties change due to pressure oscillation that supposes to be taken into consideration the results. The model of severe slugging is also limited to full blockage at the base riser, while other types of severe slugging can also occur. This point can be useful for further work to design a better model and more accurate results.

Bibliography

Agrawal, S., Gregory, G., Govier, G., 1973. An analysis of horizontal stratified two phase flow in pipes. The Canadian Journal of Chemical Engineering 51, 280–286.

Alves, I., Caetano, E., Minami, K., Shoham, O., et al., 1991. Modeling annular flow behavior for gas wells. SPE production engineering 6, 435–440.

Barnea, D., 1986. Transition from annular flow and from dispersed bubble flow—unified models for the whole range of pipe inclinations. International journal of multiphase flow 12, 733–744.

Barnea, D., Shoham, O., Taitel, Y., 1982. Flow pattern transition for downward inclined two phase flow; horizontal to vertical. Chemical Engineering Science 37, 735–740.

Bendiksen, K., Espedal, M., 1992. Onset of slugging in horizontal gas-liquid pipe flow. International journal of multiphase flow 18, 237–247.

Bendiksen, K.H., 1984. An experimental investigation of the motion of long bubbles in inclined tubes. International journal of multiphase flow 10, 467–483.

Bendiksen, K.H., Maines, D., Moe, R., Nuland, S., et al., 1991. The dynamic two-fluid model olga: Theory and application. SPE production engineering 6, 171–180.

Biberg, D., Halvorsen, G., 2000. Wall and interfacial shear stress in pressure driven two-phase laminar stratified pipe flow. International journal of multiphase flow 26, 1645–1673.

Calderbank, P., 1959. Physical rate processes in industrial fermentation. part ii—mass transfer coefficients in gas–liquid contacting with and without mechanical agitation. Trans. Inst. Chem. Eng 37, 173–185.

De Salis, J., De Marolles, C., Falcimaigne, J., Durando, P., et al., 1996. Multiphase pumping-operation & control, in: SPE Annual Technical Conference and Exhibition, Society of Petroleum Engineers.

Fuchs, P., 1997. Kompendium - fag 67173 flerfase rørstrømning .

Haaland, S.E., 1983. Simple and explicit formulas for the friction factor in turbulent pipe flow .

Hinze, J., 1955. Fundamentals of the hydrodynamic mechanism of splitting in dispersion processes. AIChE Journal 1, 289–295.

Jansen, F., Shoham, O., Taitel, Y., 1996. The elimination of severe slugging—experiments and modeling. International journal of multiphase flow 22, 1055–1072.

Kashou, S., 1996. Severe slugging in an s-shaped or catenary riser: Olga prediction and experimental verification. Advanced in Multiphase Technology .

Kristiansen, O., 2004. Experiments on the transition from stratified to slug flow in multiphase pipe flow. .

Levich, V.G., 1962. Physicochemical hydrodynamics prentice-hall. Englewood Cliffs, NJ 115.

Malnes, D., 1987. Slug flow in vertical, horizontal and inclined pipes. Institute for Energy Technology.

Mathews, J.H., Fink, K.D., et al., 2004. Numerical methods using MATLAB. volume 4. Pearson Prentice Hall Upper Saddle River, NJ.

Milne-Thomson, L.M., 1996. Theoretical hydrodynamics. Courier Corporation.

Nydal, O., 2019. Multiphase transport–tep4250, lectures notes. Norwegian University of Science and Technology .

Russell, T., Etchells, A., Jensen, R., Arruda, P., 1974. Pressure drop and holdup in stratified gas-liquid flow. AIChE Journal 20, 664–669.

Schmidt, Z., Brill, J.P., Beggs, H.D., et al., 1980. Experimental study of severe slugging in a two-phase-flow pipeline-riser pipe system. Society of Petroleum Engineers Journal 20, 407–414.

Schmidt, Z., Doty, D.R., Dutta-Roy, K., et al., 1985. Severe slugging in offshore pipeline riser-pipe systems. Society of Petroleum Engineers Journal 25, 27–38.

Shoham, O., 2005. Mechanistic Modeling Of Gas/Liquid Two-Phase Flow In Pipes. Spe.

Martins da Silva, C., Dessen, F., Nydal, O., et al., 2010. Dynamic multiphase flow models for control, in: 7th North American Conference on Multiphase Technology, BHR Group.

Taitel, Y., Bornea, D., Dukler, A., 1980. Modelling flow pattern transitions for steady upward gas-liquid flow in vertical tubes. AIChE Journal 26, 345–354.

Tengesdal, J., Sarica, C., Thompson, L., et al., 2003. Severe slugging attenuation for deepwater multiphase pipeline and riser systems. SPE production & facilities 18, 269–279.

Yocum, B., et al., 1973. Offshore riser slug flow avoidance: mathematical models for design and optimization, in: SPE European Meeting, Society of Petroleum Engineers.

Appendix

This appendix includes the python script for void fraction calculation, severe slugging model and transition velocity calculation. The script for the void fraction are presented for slug flow, annular flow, bubble flow and stratified flow. For the transition map, the slug flow stability will be used as an example to represent bisection method and velocity calculation script.

5.1 Void Fraction Calculation

5.1.1 Annular Flow

```
def annular():
    global Y, Z, voidannular, alfa_check, void_min

    #Velocity
    alfa = alfa_annular
    alfa_check=alfa
    U_l=U_sl/(1-alfa)
    U_g=U_sg/alfa

    #Geometry
    S_l=diameter*pi
    S_i=diameter*pi*(alfa)**(1/2)
    d_f=(diameter/2)*(1-alfa**(1/2))
    Dh_l=(4*(1-alfa)*A)/S_l
    Dh_g=diameter-2*d_f

    #Friction
    N_re_l=rho_l*abs(U_l)*Dh_l/vis_l
    N_re_g=rho_g*abs(U_g)*Dh_g/vis_g

    if N_re_g>4000:
        C_g=0.046
        n_g=0.2
    else:
        C_g=16
        n_g=1
    if N_re_l>4000:
        C_l=0.046
```

```
        n_l=0.2
    else:
        C_l=16
        n_l=1

    lambda_l_blasius=C_l*N_re_l**(-n_l)
    lambda_g_blasius=C_l*N_re_g**(-n_g)
    lambda_g=lambda_g_blasius
    lambda_l=lambda_l_blasius
    lambda_i=lambda_g*(1+150*(1-alfa**1/2))

    F_w=(1/2)*rho_l*lambda_l*abs(U_l)*U_l*S_l/(A)
    F_i=(1/2)*rho_g*lambda_i*abs(U_g)*(U_g)*S_i/(A)

    #Gravity
    G_l=rho_l*g*sin(phi)
    G_g=rho_g*g*sin(phi)

    #Holdup equation
    voidannular=-F_w/(1-alfa)+F_i*(1/(1-alfa)+(1/alfa))
    -(G_l-G_g)

    void_min=g*(rho_l-rho_g)*diameter*sin(phi/2)
    *(3*alfa/2-1)-1/16*C_l*rho_l*(rho_l*Dh_l/vis_l)**(-n_l)
    *(U_sl)**(2-n_l)*((1/2+3*alfa/4)/(1/2-alfa/4)**3)
```

5.1.2 Stratified Flow

```
def stratified():
    global void_strat, U_gTD, U_g, h_l, U_gKH, Usl_limit

    #Geometry
    theta=pi*(1-alfa)+(3*pi/2)*(1-2*(1-alfa)+(1-alfa)
    **(1/3)-alfa**(1/3))
    h_l=diameter*(1-cos(theta))/2

    S_l=theta*diameter
    S_g=pi*diameter-S_l
    S_i=diameter*sin(theta)

    Dh_l=(4*(1-alfa)*A)/S_l
    Dh_g=(4*(alfa)*A)/(S_g+S_i)

    #Flow
    U_l=U_sl/(1-alfa)
```

```
    U_g=U_sg/alfa

    #Taitel Duckler
    C_2=1-h_l/diameter
    A_g=alfa*A
    U_gTD=C_2*(g*(rho_l-rho_g)*A_g*cos(phi)/(rho_g*S_i))
    **0.5

    N_re_l=rho_l*abs(U_l)*Dh_l/vis_l
    N_re_g=rho_g*abs(U_g)*Dh_g/vis_g

    #Friction Haaland (page 45)
    lambda_l_haaland=(1/(1.8*log((6.9/N_re_l)+
    (eps/(3.7*Dh_l))**1.11)))**2
    lambda_g_haaland=(1/(1.8*log((6.9/N_re_g)+
    (eps/(3.7*Dh_g))**1.11)))**2

    lambda_g=max(lambda_g_haaland,64/N_re_g)
    lambda_l=max(lambda_l_haaland,64/N_re_l)

    lambda_i_haaland=lambda_g
    lambda_i=(lambda_i_haaland)

    F_l=rho_l*lambda_l*abs(U_l)*U_l*S_l/(8*A)
    F_g=rho_g*lambda_g*abs(U_g)*U_g*S_g/(8*A)
    F_i=rho_g*lambda_i*abs(U_g-U_l)*(U_g-U_l)*S_i/(8*A)

    #Gravity
    G_l=(1-alfa)*rho_l*g*sin(phi)
    G_g=alfa*rho_g*g*sin(phi)

    #Holdup equation
    void_strat=F_i+(1-alfa)*F_g-alfa*F_l-alfa*(1-alfa)
    *sin(phi)*(rho_l-rho_g)
```

5.1.3 Bubble Flow

```
def bubble():
    global d_max, d_cb, d_cd, check_null, alfa

    U_m=U_sl+U_sg
    alfa=U_sg/U_m

    rho_m=alfa*rho_g+(1-alfa)*rho_l
    vis_m=alfa*vis_g+(1-alfa)*vis_l
```

```
    N_re_m=rho_m*abs(U_m)*diameter/vis_m

    if N_re_m>4000:
        C_m=0.046
        n_m=0.2
    else:
        C_m=16
        n_m=1

    lambda_m_blasius=C_m*N_re_m**(-n_m)

    lambda_m=lambda_m_blasius

    epsilon=2*lambda_m*U_m**3/diameter

    d_max=(0.725+4.15*alfa**0.5)*(sigma/rho_l)
    **0.6*(epsilon)**-0.4
    d_cd=2*(0.4*sigma/((rho_l-rho_g)*g))**0.5
    d_cb=(3/8)*(rho_l/(rho_l-rho_g))
    *(lambda_m*U_m**2)/(g*cos(phi))

    #there are 2 other equation
    A=1.53*(g*sigma*(rho_l-rho_g)/rho_l**2)**(1/4)
    *(1-alfa)**0.5*sin(phi)
    B=U_sg/alfa-1.2*U_m
    check_null=A-B
```

5.1.4 Slug Flow

```
def slug():
    global H_slug, SF, U_t, U_gs, U_ls, alfa_s

    #void fraction slug
    alfa_s= (U_sg+U_sl)/(83*(g*sigma/rho_l)
    **0.25+(U_sg+U_sl))

    #slip relation
    S_D=(1-alfa_s)/(0.95-alfa_s) #distribution
    U_os=1.18*(g*sigma*(rho_l-rho_g)/rho_l**2)
    **(1/4)*(1-alfa_s)**(1/2)#rising velocity of gas
    U_ls=((U_sg+U_sl)-S_D*alfa_s*U_os)/
    (alfa_s*(S_D-1)+1)

    U_gs=S_D*(U_ls+U_os)
```

```
    U_ov=0.35*(g*diameter*(rho_l-rho_g)/rho_l)**(1/2)
    U_oh=0.54*(g*diameter*(rho_l-rho_g)/rho_l)**(1/2)

    Fr_lim=3.6
    Fr=(U_sg+U_sl)/(g*diameter
    *(rho_l-rho_g)/rho_l)**0.5

    C_o_1=1.05+0.15*(sin(phi))**2
    U_o_1=-U_ov*sin(phi)+U_oh*cos(phi)
    U_b_1=C_o_1*(U_sg+U_sl)+U_o_1

    C_o_2=1.2
    U_o_2=-U_ov*sin(phi)
    U_b_2=C_o_2*(U_sg+U_sl)+U_o_2

    U_b=max(U_b_1, U_b_2)
    U_t=U_b

    #find alfa_b from stratified holdup equation
    bisectvoid_bubble_slug()

    #bubble velocity
    U_gb=U_t-(alfa_s/alfa_b)*(U_t-U_gs)
    U_lb=U_t-((1-alfa_s)/(1-alfa_b))*(U_t-U_ls)

    #slug geometry
    SF=1-(U_sg-U_gs*alfa_s)/(U_t*(alfa_b-alfa_s))
    H_slug=SF*(1-alfa_s)+(1-SF)*(1-alfa_b)
```

5.2 Transition Map

In this chapter only bisection method for slug flow script will be presented. For other flow regime transition such as stratified stability, the calculation routine that need to be change are criteria to determine U_{sl} during transition.

5.2.1 Bisection Method

```
def bisectvoid_strat():
    global alfa
    data()
    x=0.5
    dx=diameter/10
    tol=1e-5
    a=x-dx
```

```
alfa=a
stratified()
fa=void_strat
b=x+dx
alfa=b
stratified()
fb=void_strat
count=0
countmax=100
while (fa > 0)==(fb > 0):
    count=count+1
    dx=dx*2
    a=x-dx
    a=max(a,1e-6)
    alfa=a
    stratified()
    fa=void_strat
    if (fa > 0)!=(fb > 0):
        break
    if count>=countmax:
        break
    b=x+dx
    b=min(0.99999,b)
    alfa=b
    stratified()
    fb=void_strat
count=0
while abs(b-a) > 2.0*tol*max(abs(b),1.0):
    c=a+0.5*(b-a)
    alfa=c
    stratified()
    fc=void_strat
    count=count+1
    if (fb > 0)==(fc > 0):
        b=c
        fb=fc
    else:
        a=c
        fa=fc
    if count>=countmax:
        break
alfa=b
```

5.2.2 Velocity Calculation

```
def test_bendiksen_espedal_1(): #4 (SF=0)
    global lowerbound, higherbound, U_sl

    Accuracy=1e-5
    lowerbound=Usl_min_input
    higherbound=5
    countmax=100
    count=0
    while ((higherbound - lowerbound) > Accuracy ):
        count=count+1
        U_sl= 0.5*(lowerbound+higherbound)
        slug()
        bisectvoid_strat()
        H_strat=1-alfa
        if count>=countmax:
            break
        if H_slug>=H_strat:  #no slug
            lowerbound=U_sl
        else:
            higherbound=U_sl

def maptrans_bendiksen_espedal_1(): #4
    global bendiksen_1_Usl, bendiksen_1_Usg, U_sg
    data()
    bendiksen_1_Usg=[0]*Usg_step_input
    bendiksen_1_Usl=[0]*Usg_step_input
    dx=(Usg_max_input-Usg_min_input)/Usg_step_input
    U_sg=Usg_min_input
    for i in range(0,nstep):
        U_sg=U_sg+dx
        test_bendiksen_espedal_1()
        U_sl= 0.5*(lowerbound+higherbound)
        if U_sl<0:
            bendiksen_1_Usl[i]=0
        else:
            bendiksen_1_Usl[i]=U_sl
        bendiksen_1_Usg[i]=U_sg
```

5.3 Severe Slugging Stability

5.3.1 Severe Slugging Unit

```
def slug_boundary():
    global p_max_ratio, usg_r_max, usl_r_max
    data()
```

```
Nstep=30000
DeltaT=0.01
p_res_boundary=[0]*Nstep
usg_r_res=[0]*Nstep
usl_r_res=[0]*Nstep

#pipe geometry
D=diameter
A=pi*D**2/4
sinangle=sin(phi)

#Properties
Lambda=0.05
Rog_r=rho_g
Rol=rho_l
visl=vis_l

#Slip
S=1.2
uo=0.35*sqrt(9.81*D)

#Initial value
Rom=Rol
alfa_r=0
p=p_out+Rom*9.81*L_r
p_bend=p_out
z=0.0001
U_level=0
Ug_r=0
Um=Uslin_boundary
Rog_l=p/RT

for i in range(0,Nstep):
    #Start SlugStep

    #Friction
    Re=Rol*abs(Um)*D/visl

    #Friction Haaland (page 45)
    lambda_haaland=(1/(1.8*log((6.9/Re)
    +(eps/(3.7*D))**1.11)))**2
    #Friction Blasius
    lambda_blasius=0.046*(Re)**0.2
    lambda_blasius=max(lambda_blasius,64/Re)
    #Friction Moody
```

```
lambda_moody=0.0055*(1+(2*1e4*(eps/D)
+1e6/Re)**(1/3))
lambda_moody=max(lambda_moody,64/Re)

Lambda=lambda_haaland#*(fric==2)
+lambda_blasius
*(fric==1)+lambda_moody*(fric==0)

Fric=0.5*Lambda*Rol*Um*abs(Um)
*(-z+(1-alfa_r)*L_r)/D
Lambda_stagnant=10
Fric_stagnant=0.5*Lambda_stagnant*Rol*U_level
*abs(U_level)*(-z+(1-alfa_r)*L_r)/D

#Valve Friction
Fric_valve=without_pid*Rol*Um*abs(Um)

Fric=Fric+Fric_stagnant

#Gravity
Grav_l=-Rol*9.81*abs(z*sinangle)
Grav_r=Rom*9.81*L_r
Grav=Grav_l+Grav_r

#Simplification Variable (1)
LRo=-z*Rol+L_r*Rom

#U's Value
Um_old=Um
Um=Um_old+DeltaT*((p-p_out)-Fric-Grav
-Fric_valve)/LRo

Ug_r=S*Um+uo

Usg_l=(Um-Uslin_boundary)*(Um>0)*(z>0)
Usl_l=(Uslin_boundary*(z>0)
+Um*(z<0))*(Um>0)+Um*(Um<0)
Usg_r=(alfa_r*Ug_r*(z>0)
+Um*(z<0))*(Um>0)+Um*(Um<0)
Usl_r=(Um-alfa_r*Ug_r)*(Um>0)*(z>0)

U=Usg_l-Usg_r-Usl_l+Usl_r

#Alfa Value
alfa_r_old=alfa_r
```

```
        alfa_r=alfa_r_old+0.5*DeltaT*U/(-z+L_r)

        alfa_r=max(0,alfa_r)
        alfa_r=min(1,alfa_r)

        #Gas Properties
        Rog_l=p/RT

        #Real Volume
        L_g=L_l+z

        #Level
        U_level=(-Uslin_boundary+Um)
        z_old=z
        z=z_old+DeltaT*U_level
        dHdt=((1-alfa_r)-(1-alfa_r_old))/DeltaT
        z=(z<0)*z+(z>0)*EPS
        U_level=U_level*(z<0)

        #Pressure Value
        p_old=p
        p=p_old+DeltaT*(Usgin_boundary
        *Pnormal-Usg_l*p_old)/L_g-DeltaT
        *(p_old*U_level)/L_g

        #Mixture Density
        Rog_r=Rog_l
        Rom=alfa_r*Rog_r+(1-alfa_r)*Rol
        p_res_boundary[i]=p
        usg_r_res[i]=Usg_r
        usl_r_res[i]=Usl_r
    p_res_half_mean=statistics.mean
    (p_res_boundary[12500:25000])
    p_max_ratio=max(p_res_boundary[12500:25000])
    /p_res_half_mean-1
    usg_r_max=max(usg_r_res[10000:30000])
    usl_r_max=max(usl_r_res[10000:30000])
```

5.3.2 Bisection Method

```
def boundary():
    global transition_Usg, transition_Usl, Usgin_boundary,
    Uslin_boundary, nUsl_lines
    #start
    nUsl_lines=10
```

```
Usl_step=(10-0)/10
Usg_step=1
Usl_boundary=0
transition_Usg=[0]*nUsl_lines
transition_Usl=[0]*nUsl_lines
for n in range (0,nUsl_lines):
    Usl_boundary=Usl_boundary+Usl_step
    tol=0.01
    Usg_arg=1
    dUsg_arg=Usg_step
    Usl_arg=Usl_boundary
    countMax=20
    c=0
    dx=dUsg_arg
    x=Usg_arg
    a=x
    Usgin_boundary=a
    Uslin_boundary=Usl_arg
    slug_boundary()
    fa=p_max_ratio-0.1
    b=x+dx
    Usgin_boundary=b
    Uslin_boundary=Usl_arg
    slug_boundary()
    fb=p_max_ratio-0.1
    count=0
    while (fa>0)==(fb>0):
        a=b
        b=b+dx
        Usgin_boundary=b
        Uslin_boundary=Usl_arg
        slug_boundary()
        fb=p_max_ratio-0.1
        if (fa>0)!=(fb>0):
            break
        count=count+1
        if (count>countMax):
            break
    count=0
    while abs (b-a)>2*tol*max(abs(b),1):
        c=a+0.5*(b-a)
        Usgin_boundary=c
        Uslin_boundary=Usl_arg
        slug_boundary()
        fc=p_max_ratio-0.1
```

```
        if (fb>0)==(fc>0):
            b=c
            fb=fc
        else:
            a=c
            fa=fc
        count=count+1
        if (count>countMax):
            break
        Usg_boundary=c
    transition_Usg[n]=Usg_boundary
    transition_Usl[n]=Usl_boundary
```

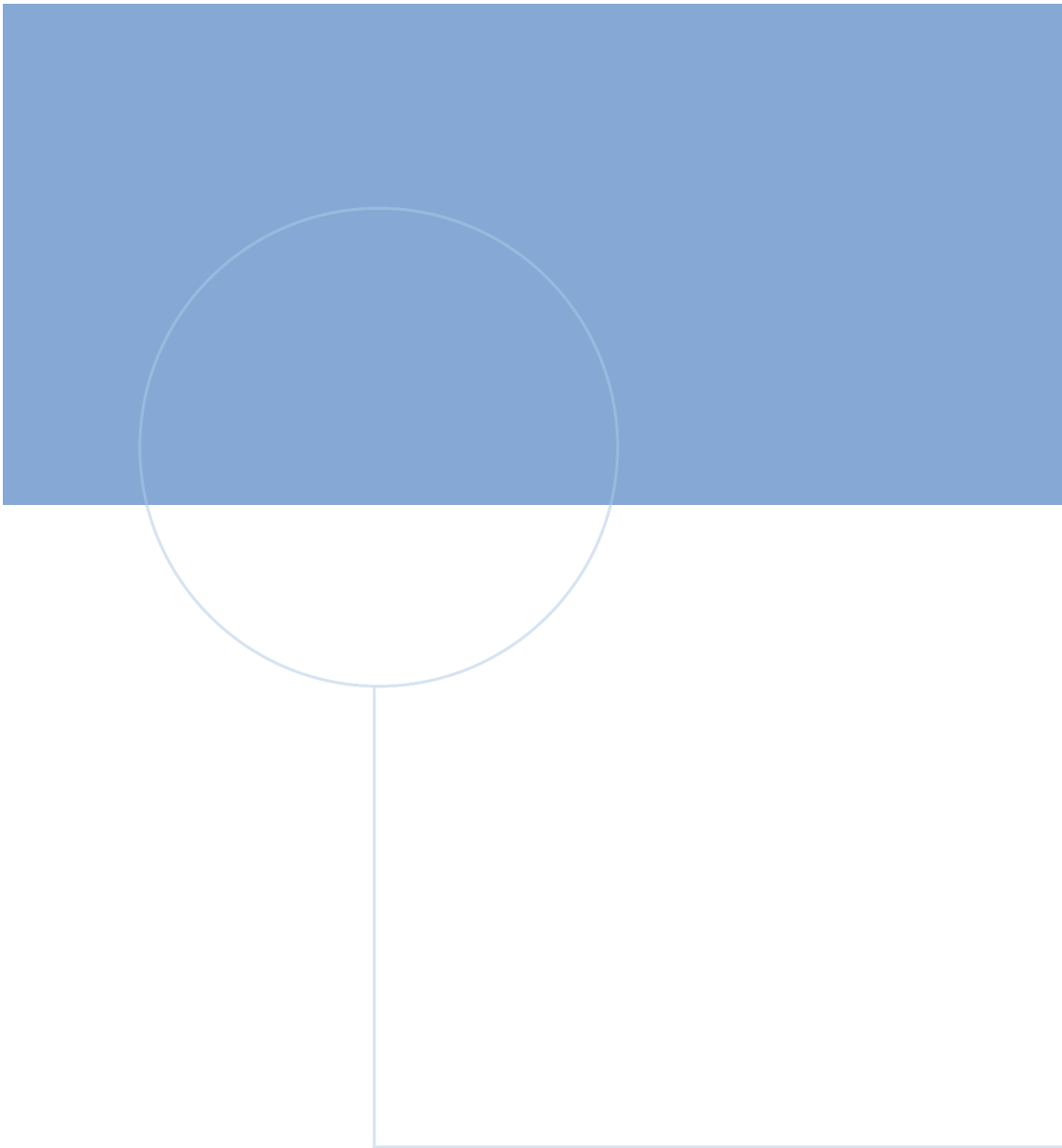

NTNU

Norwegian University of
Science and Technology